Supporting information

A novel benzothiazole-1,2,3-triazole-based arene osmium(II) complex as an effective rhabdomyosarcoma cancer stem cell agent

Sofia Sharkawy,‡ [a,b], Alba Hernández-García,‡[c] Hana Kostrhunova,[a] Delia Bautista,[d] Lenka Markova,[a] María Dolores Santana,[c] Jana Kasparkova,[a,e] Viktor Brabec,*[a,e] Jose Ruiz*[c]

[a]*Czech Academy of Sciences, Institute of Biophysics, CZ-61200 Brno, Czech Republic;*
[b]*Faculty of Science, Department of Biochemistry, Masaryk University, CZ-62500 Brno, Czech Republic;*
[c]*Departamento de Química Inorgánica, Universidad de Murcia, and Murcia BioHealth Research; Institute (IMIB-Arrixaca), E-30100 Murcia, Spain;*
[d]*ACTI, Universidad de Murcia, Murcia E-30100, Spain*
[e]*Department of Biophysics, Faculty of Science, Palacky University, Slechtitelu 27, 783 71 Olomouc, Czech Republic*

‡ These authors contributed equally to this work.
* Corresponding authors

Table of contents

1. Synthetic routes S1
2. Nuclear Magnetic Resonance (NMR) S2
3. Mass spectrometry S10
4. High performance liquid chromatography (HPLC) analysis S14
5. X-Ray diffraction S16
6. Photophysical properties S22
7. Stability studies S23
8. Interaction with Biomacromolecules S34
9. Biological assays S39

1. Synthetic routes

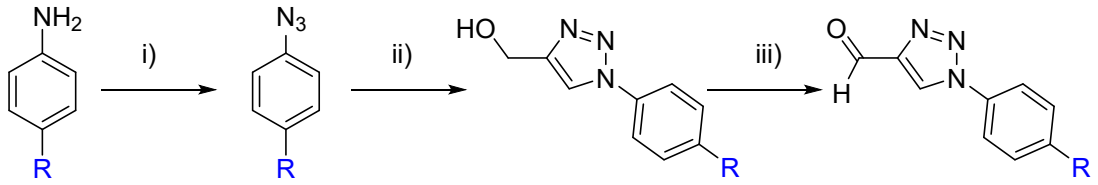

R= -Me (**L1**), -F (**L2**), -CF_3 (**L3**), -NO_2 (**L4**), -NMe_2 (**L5**)

Scheme S1. Synthetic route to obtain the aldehydes. **i)** 1) $NaNO_2$, HCl_{conc}, H_2O, 0 ºC, 1 h; 2) NaN_3, H_2O, 0º C, 15 min; 3) r.t., 2 h. **ii)** Propargyl alcohol, $CuSO_4 \cdot 5H_2O$ (5% mol), sodium ascorbate (10% mol), ^tBuOH /H_2O (1:1), r.t., 72 h. **iii)** 1) $(COCl)_2$, DMSO, DCM, -78 ºC, atm., N_2, 15 min; 2) DCM, -78 ºC, atm. N_2, 15 min; 3) Et_3N, atm N_2, -78 ºC, 15 min, r.t., 24 h.

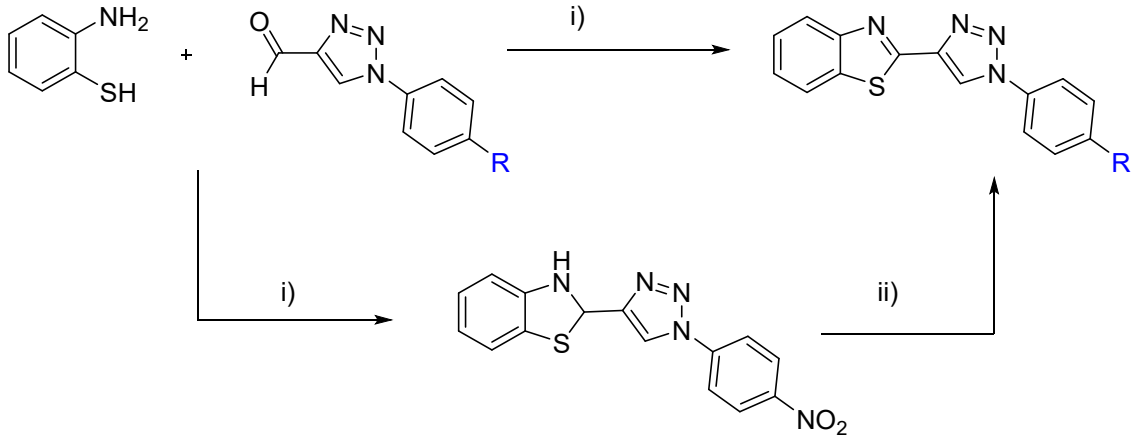

R= -Me (**L1**), -F (**L2**), -CF_3 (**L3**), -NO_2 (**L4**), -NMe_2 (**L5**)

Scheme S2. Synthetic route to obtain the ligands. i) CF_3COOH (5 % mol) EtOH, r.t., 24 h. ii) DDQ, DCM, 0 ºC, 2 h.

2. Nuclear Magnetic Resonance (NMR)

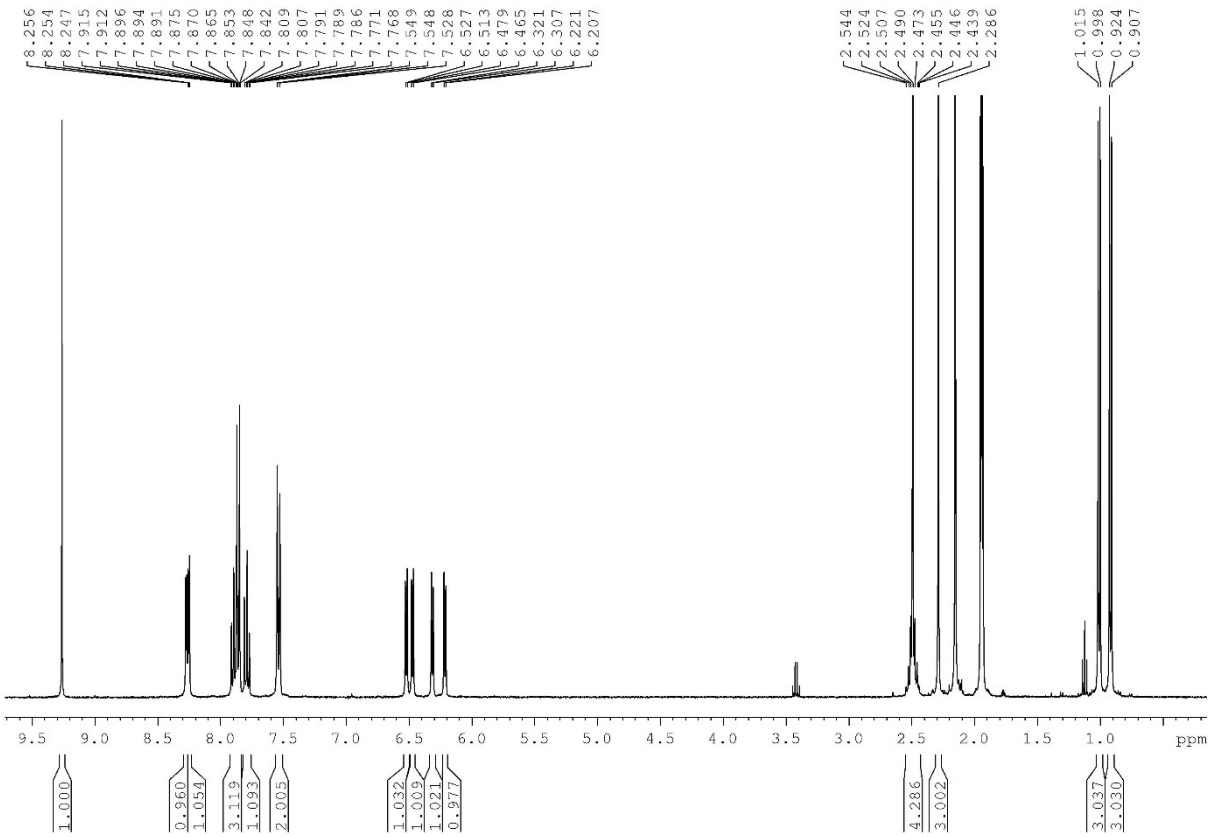

Figure S1. ^{1}H NMR of **Os1** in CD_3CN.

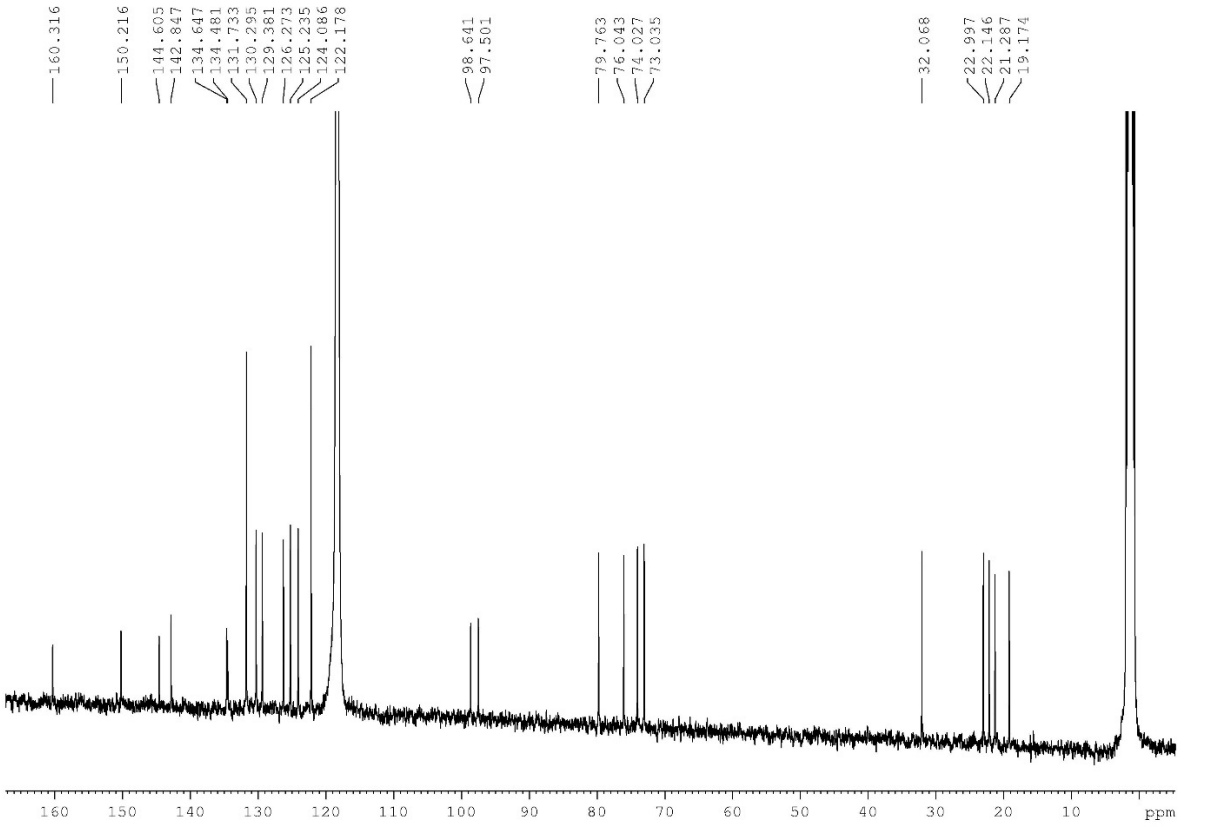

Figure S2. ^{13}C NMR of **Os1** in CD_3CN.

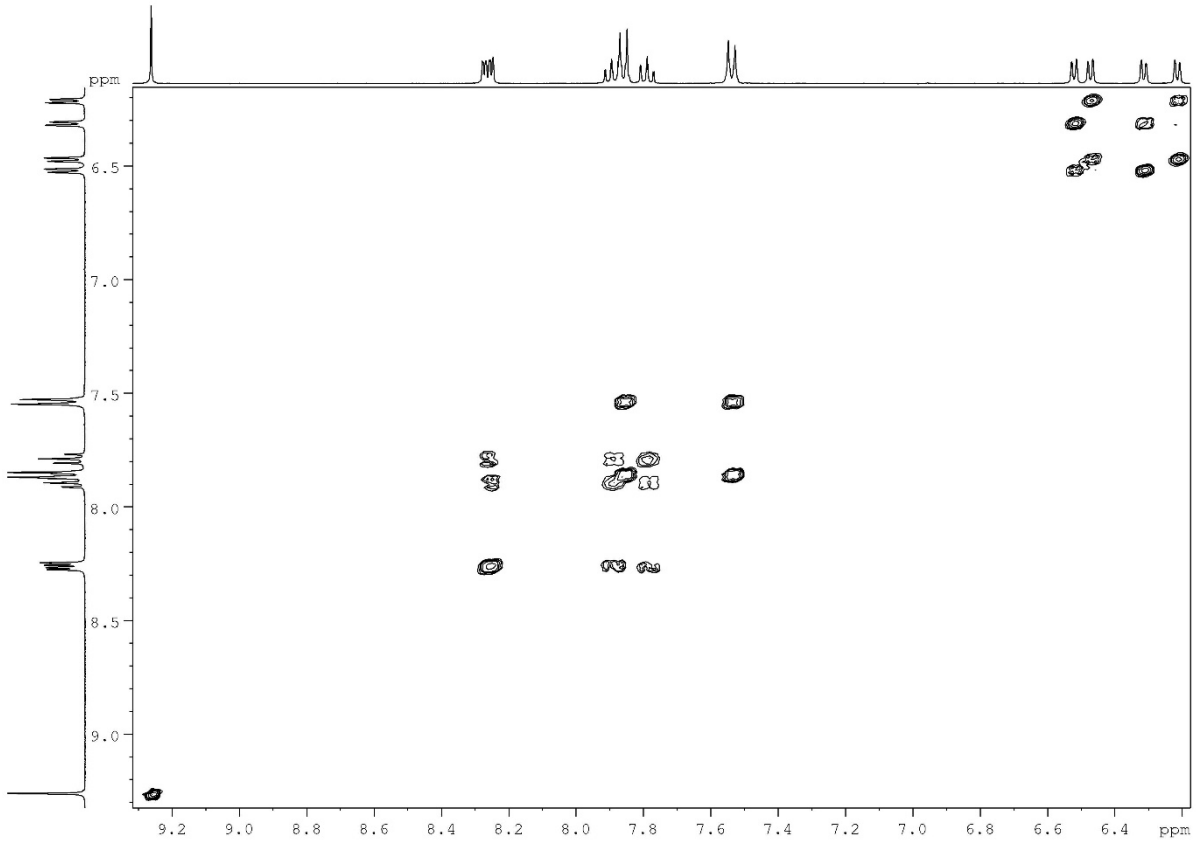

Figure S3. ^{1}H-^{1}H COSY NMR spectrum of **Os1** in CD_3CN.

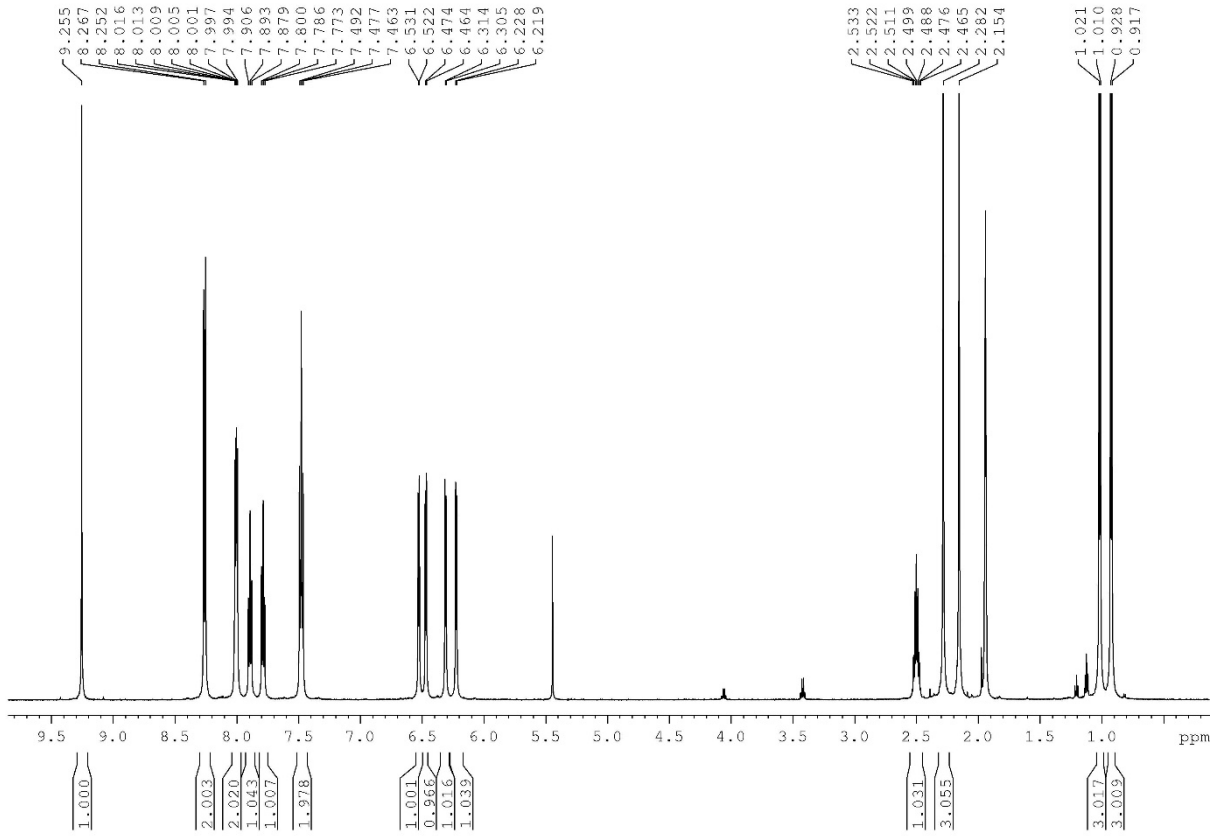

Figure S4. ^{1}H NMR of **Os2** in CD_3CN.

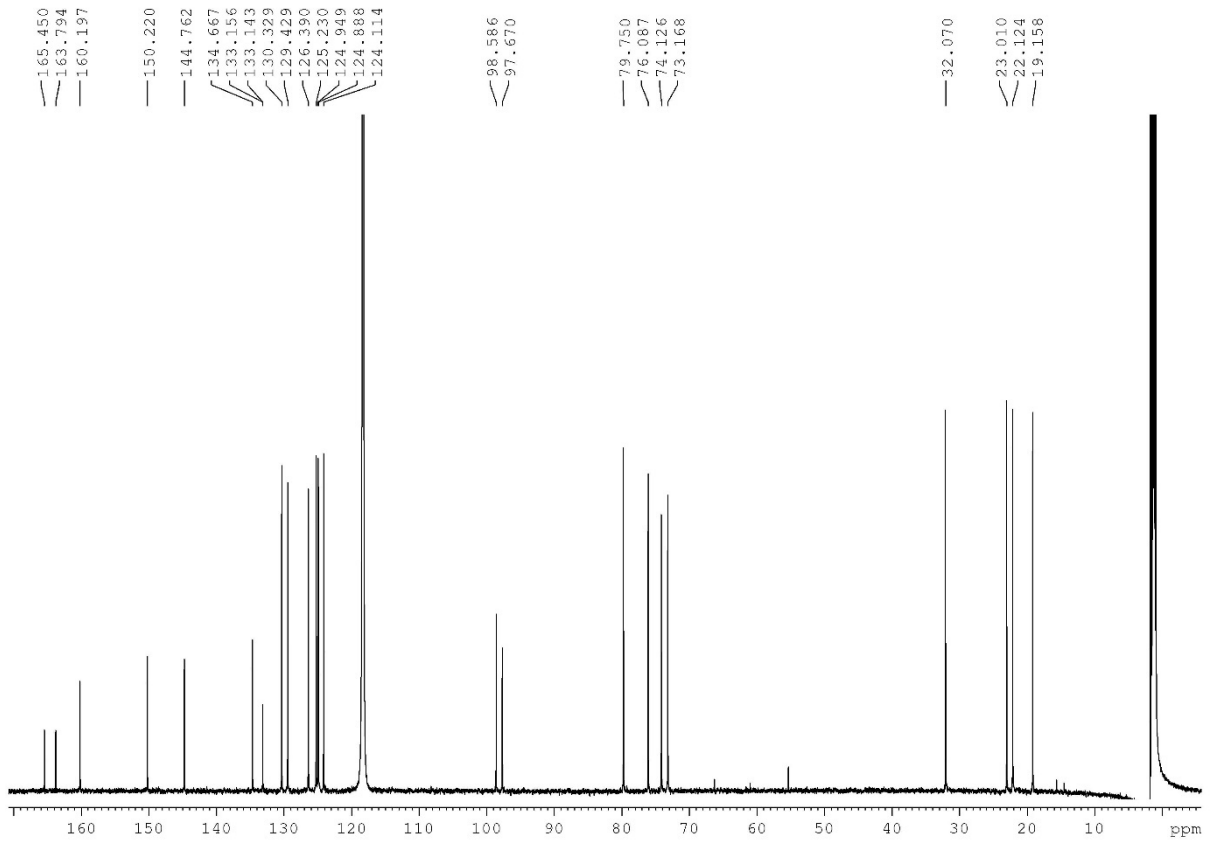

Figure S5. ^{13}C NMR of **Os2** in CD_3CN.

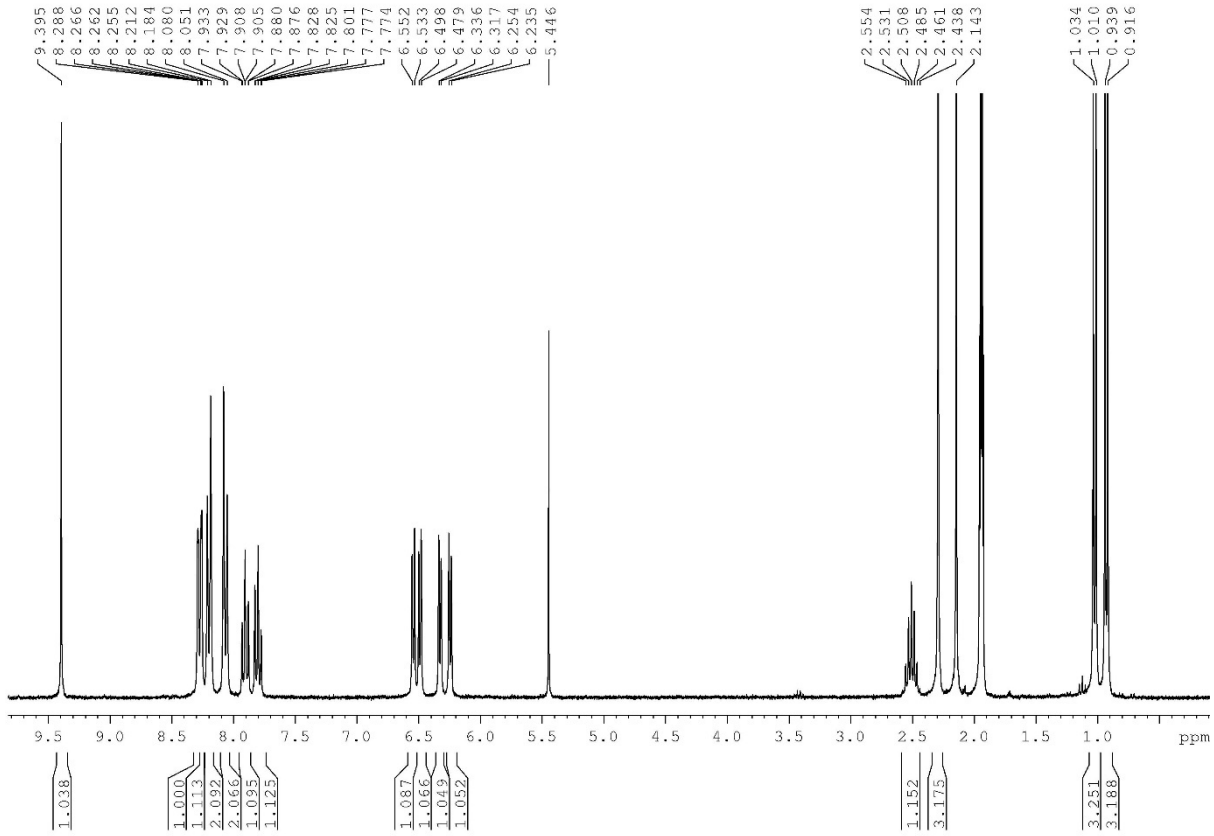

Figure S6. ^{1}H-NMR of **Os3** in CD_3CN.

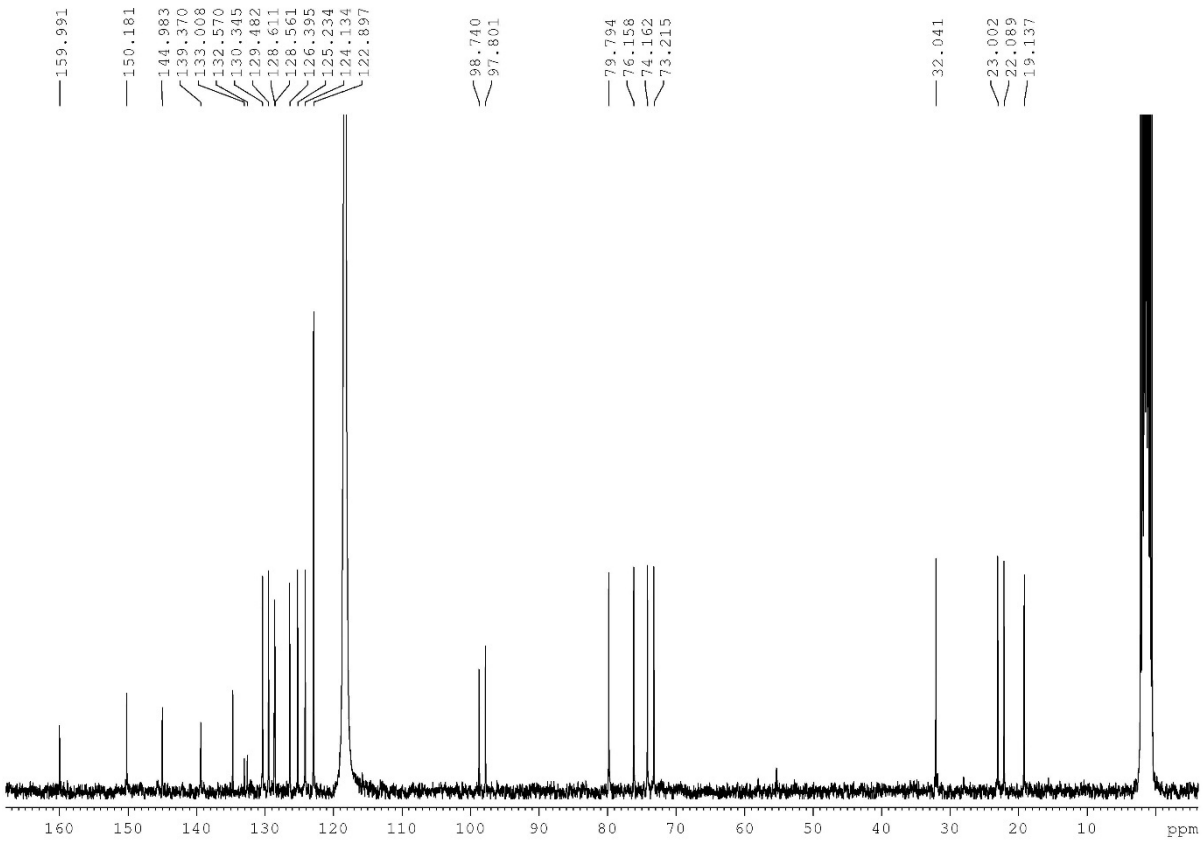

Figure S7. ^{13}C NMR spectrum of **Os3** in CD_3CN.

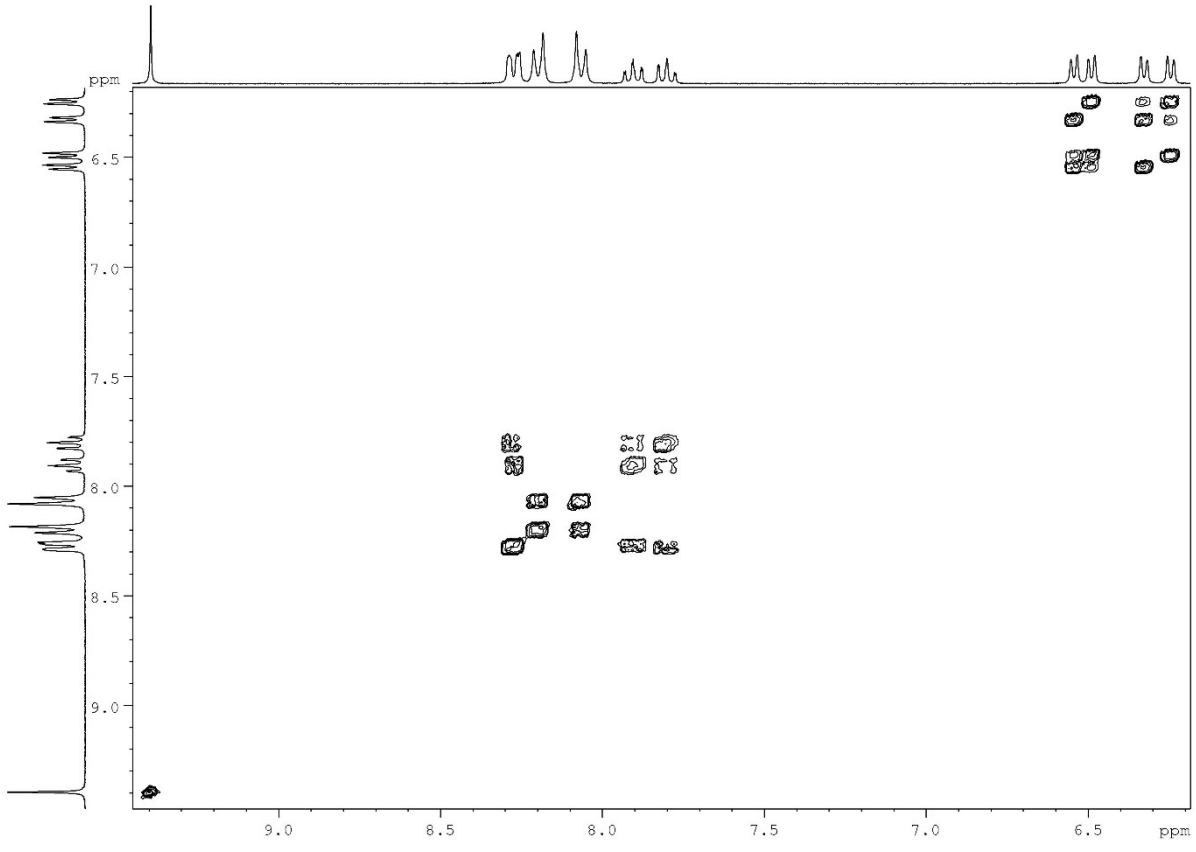

Figure S8. ^{1}H-^{1}H COSY NMR spectrum of **Os3** in CD_3CN.

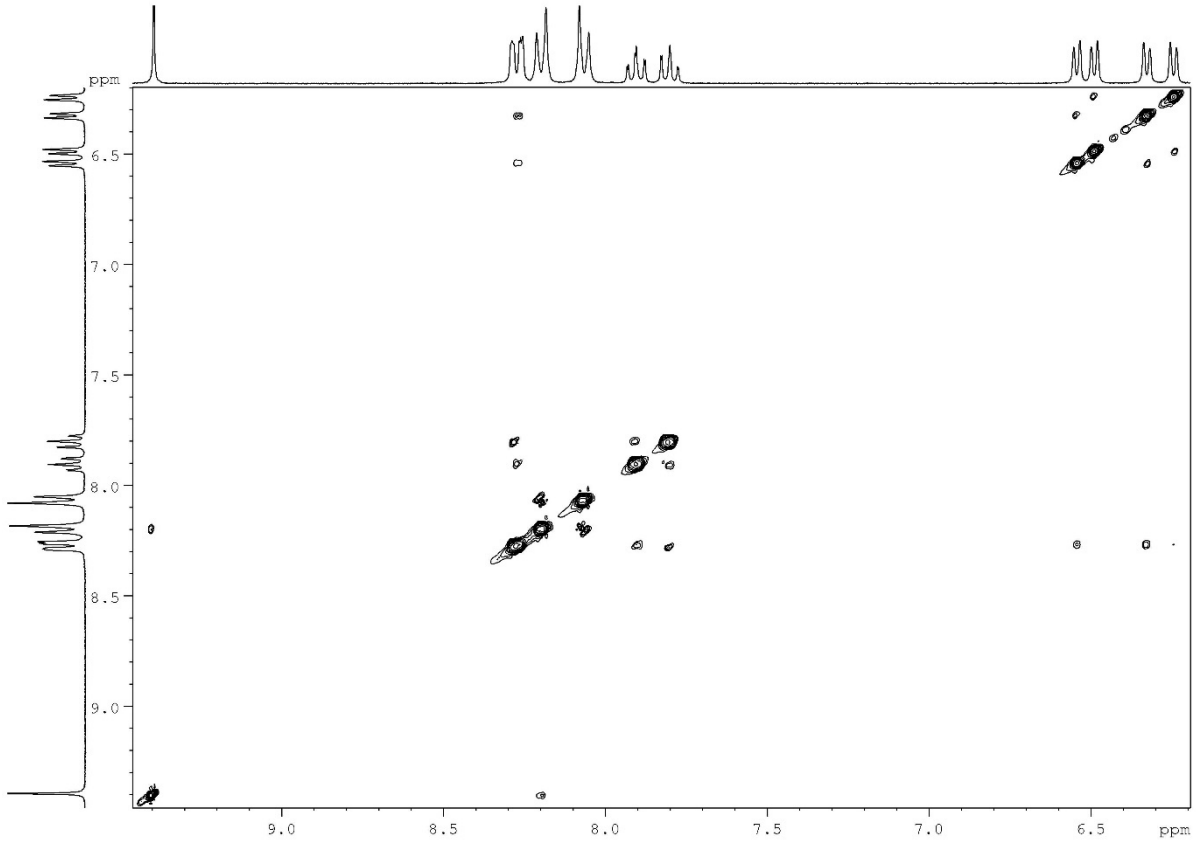

Figure S9. ^{1}H-^{1}H NOESY NMR spectrum of **Os3** in CD_3CN.

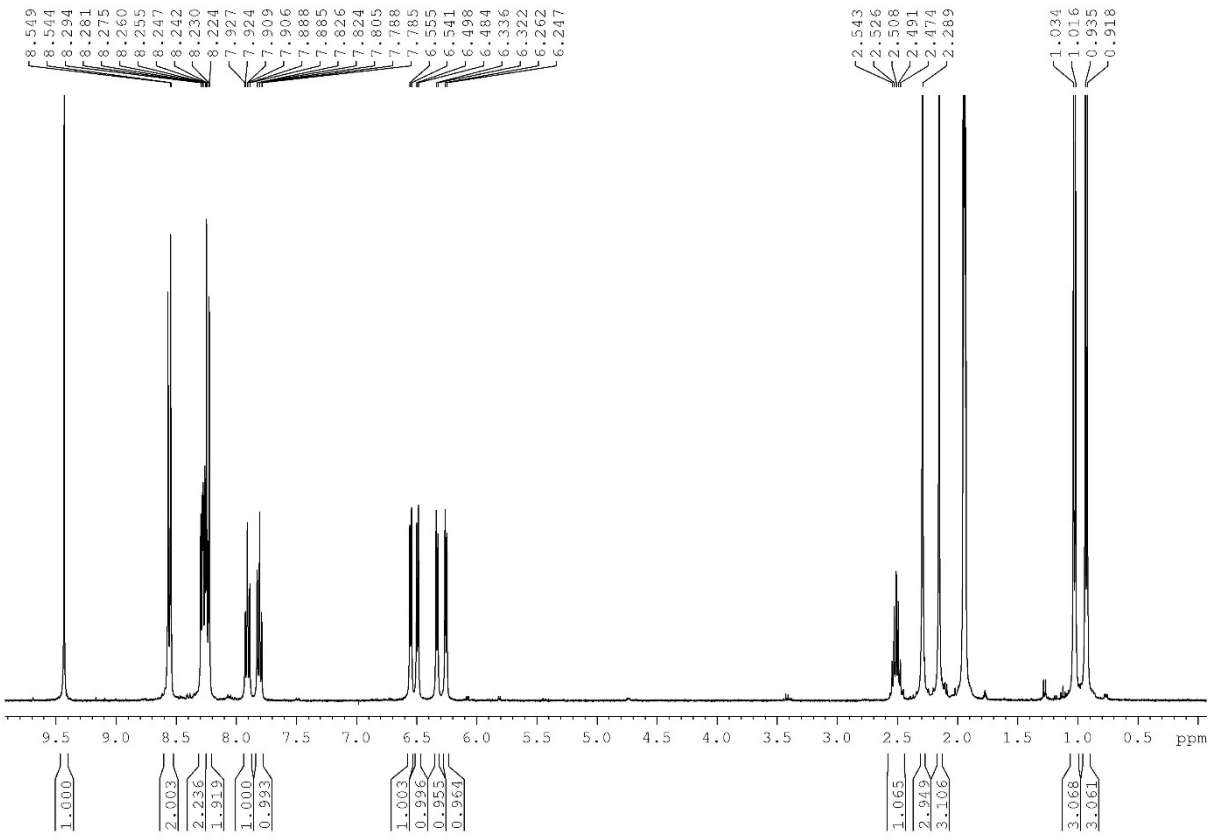

Figure S10. ^{1}H-NMR spectrum of **Os4** in CD_3CN.

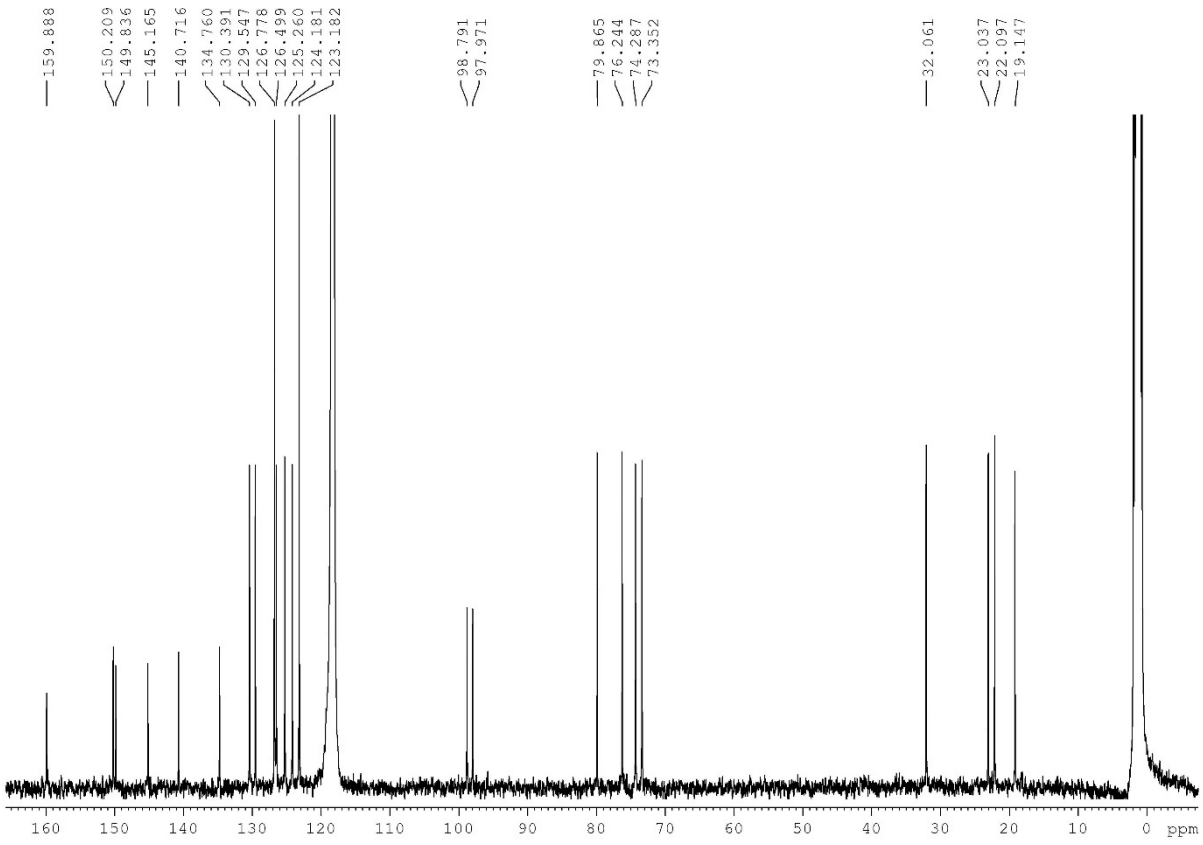

Figure S11. ^{13}C NMR spectrum of **Os4** in CD_3CN.

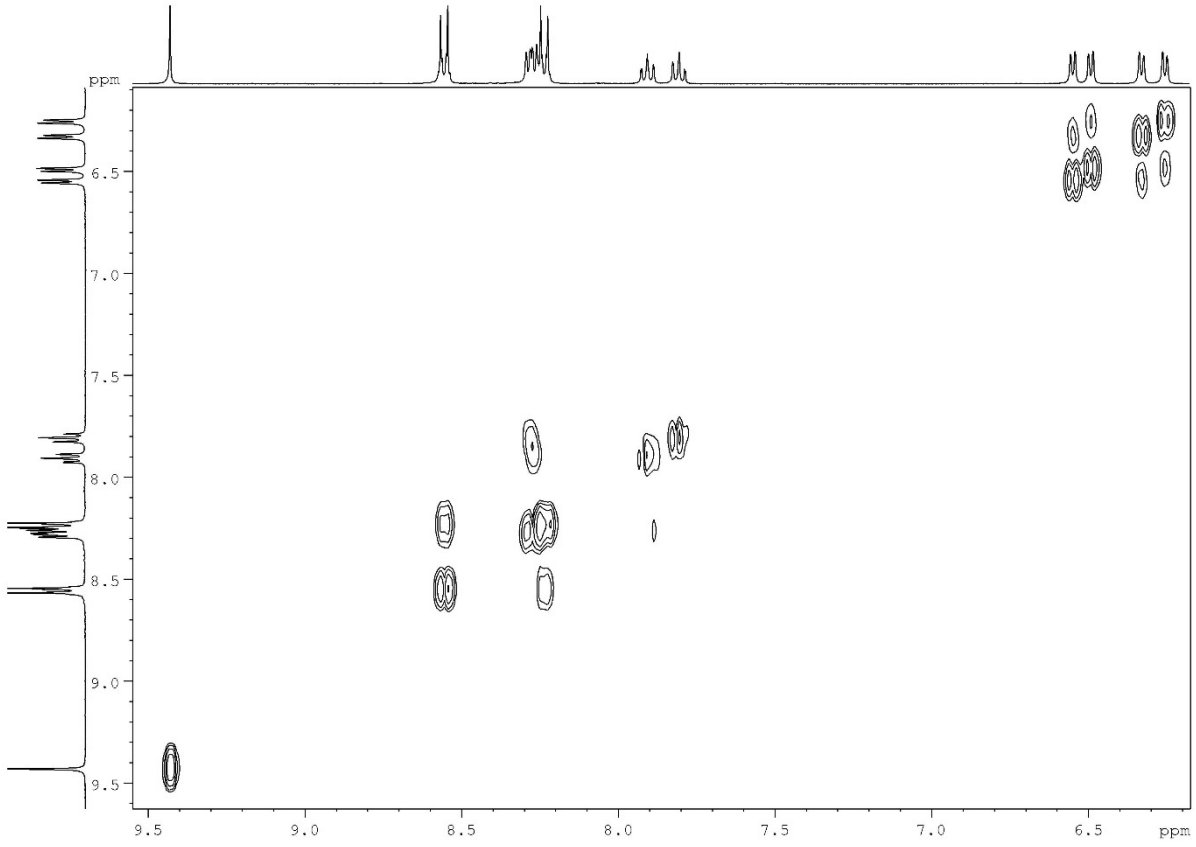

Figure S12. ^{1}H-^{1}H COSY NMR spectrum of **Os4** in CD_3CN.

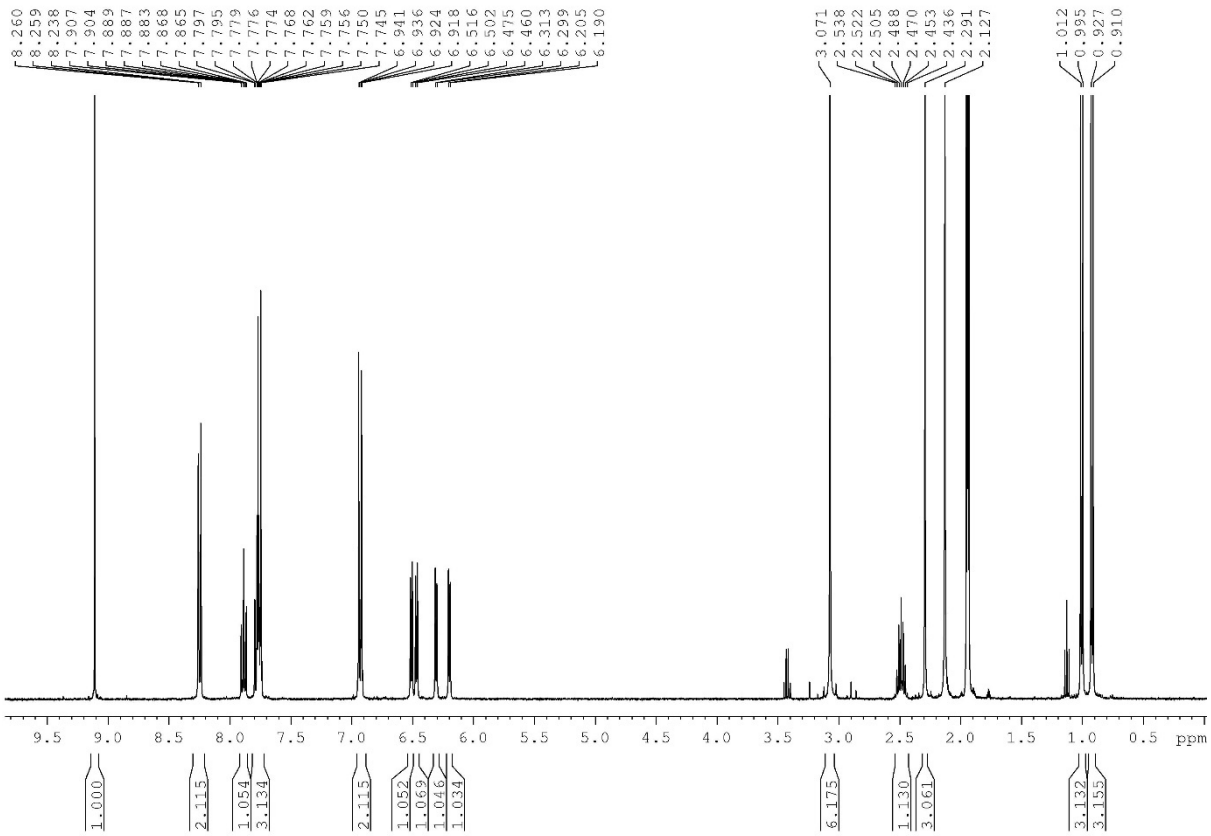

Figure S13. ^{1}H-NMR of **Os5** in CD_3CN.

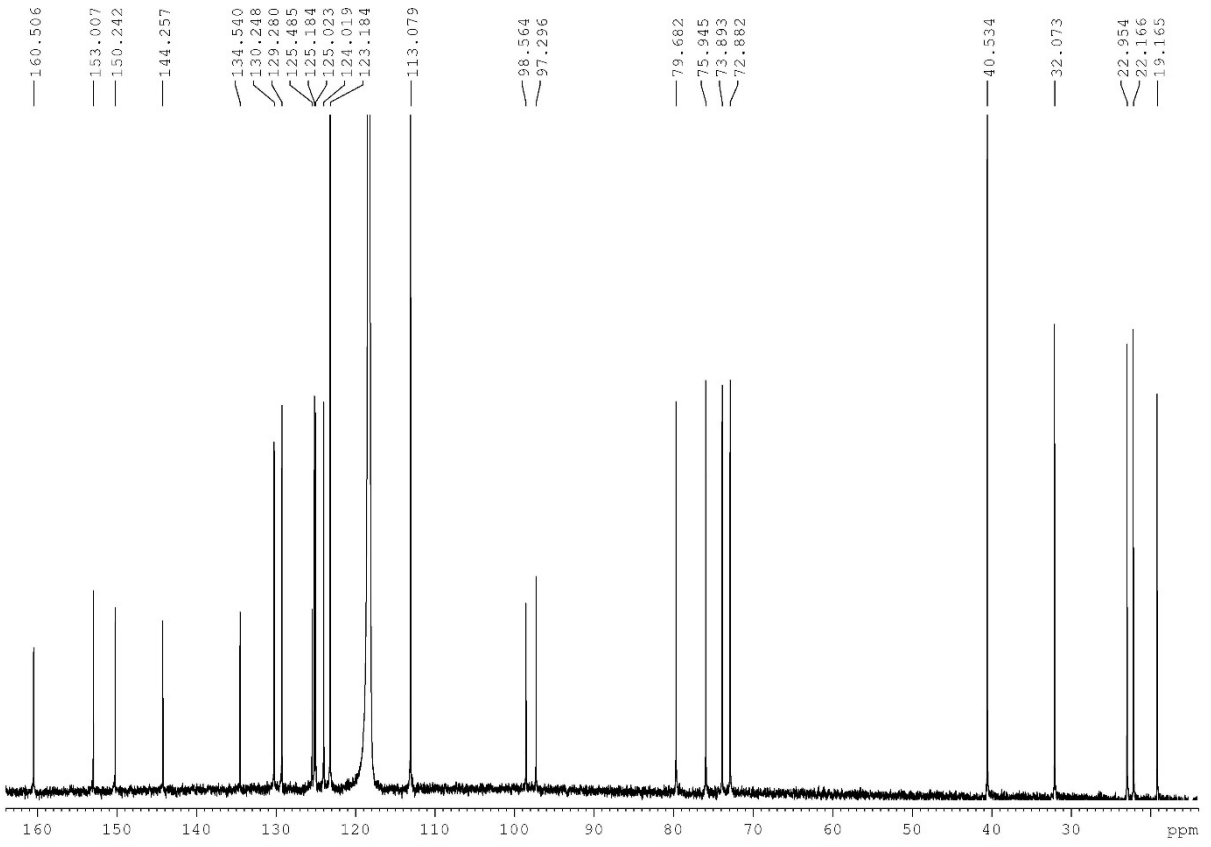

Figure S14. ^{13}C NMR spectrum of **Os5** in CD_3CN.

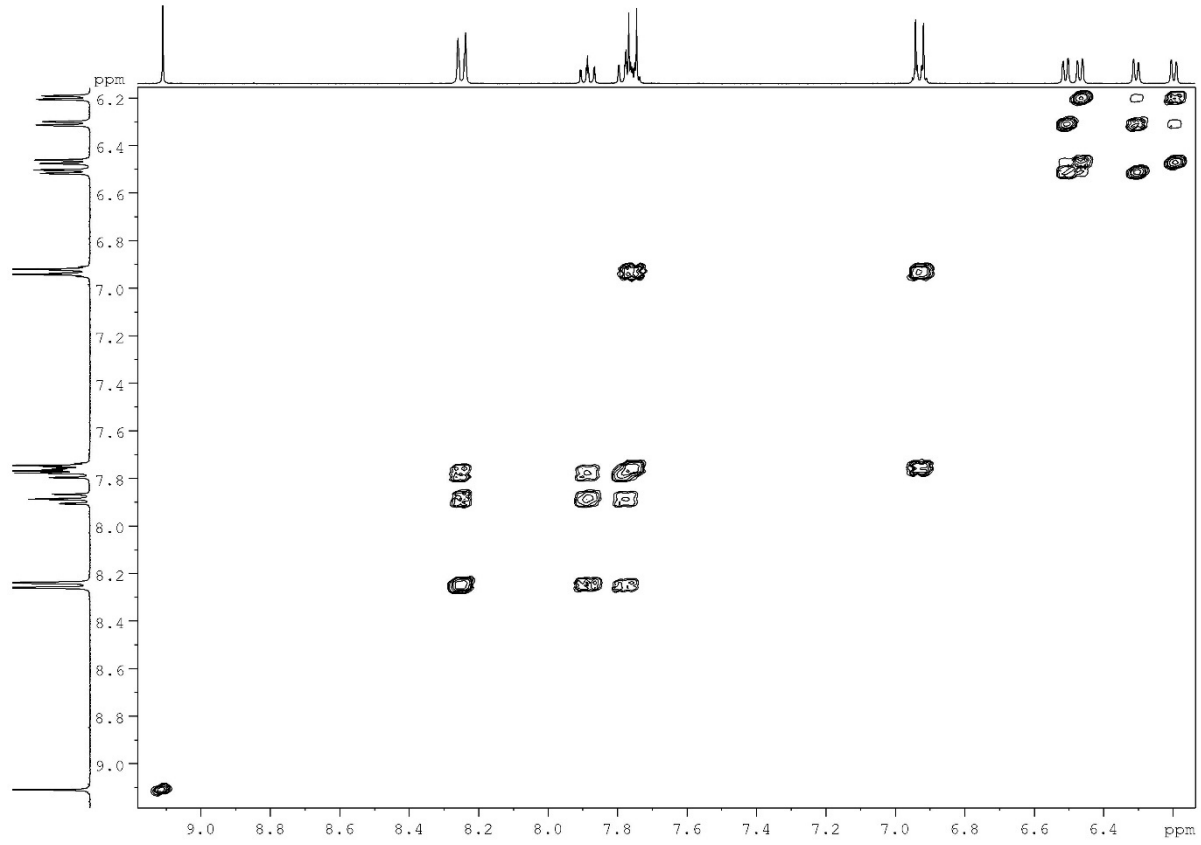

Figure S15. ^{1}H-^{1}H COSY NMR spectrum of **Os5** in CD_3CN.

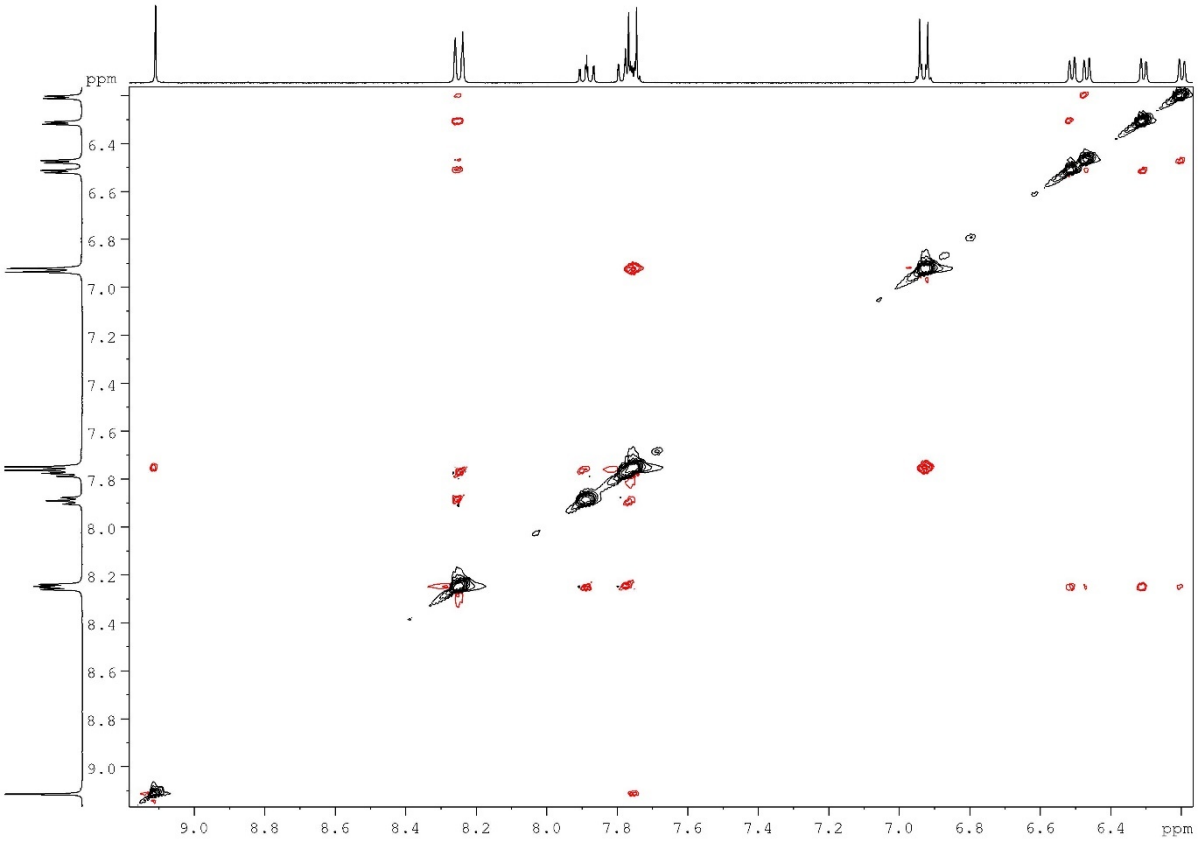

Figure S16. ^{1}H-^{1}H NOESY NMR spectrum of **Os5** in CD_3CN.

3. Mass spectrometry

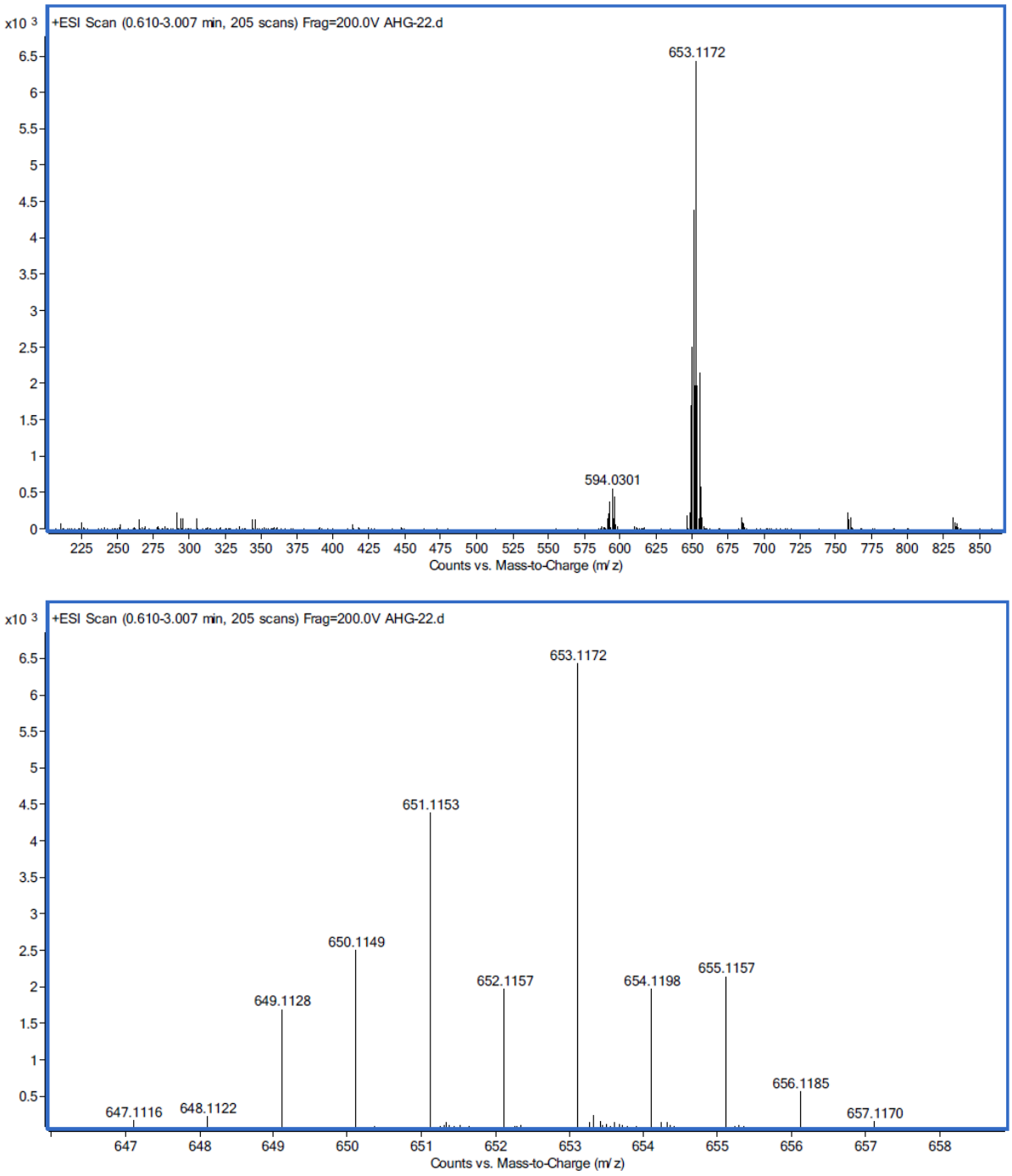

Figure S17. ESI-HRMS spectrum of complex **Os1** (positive detection mode).

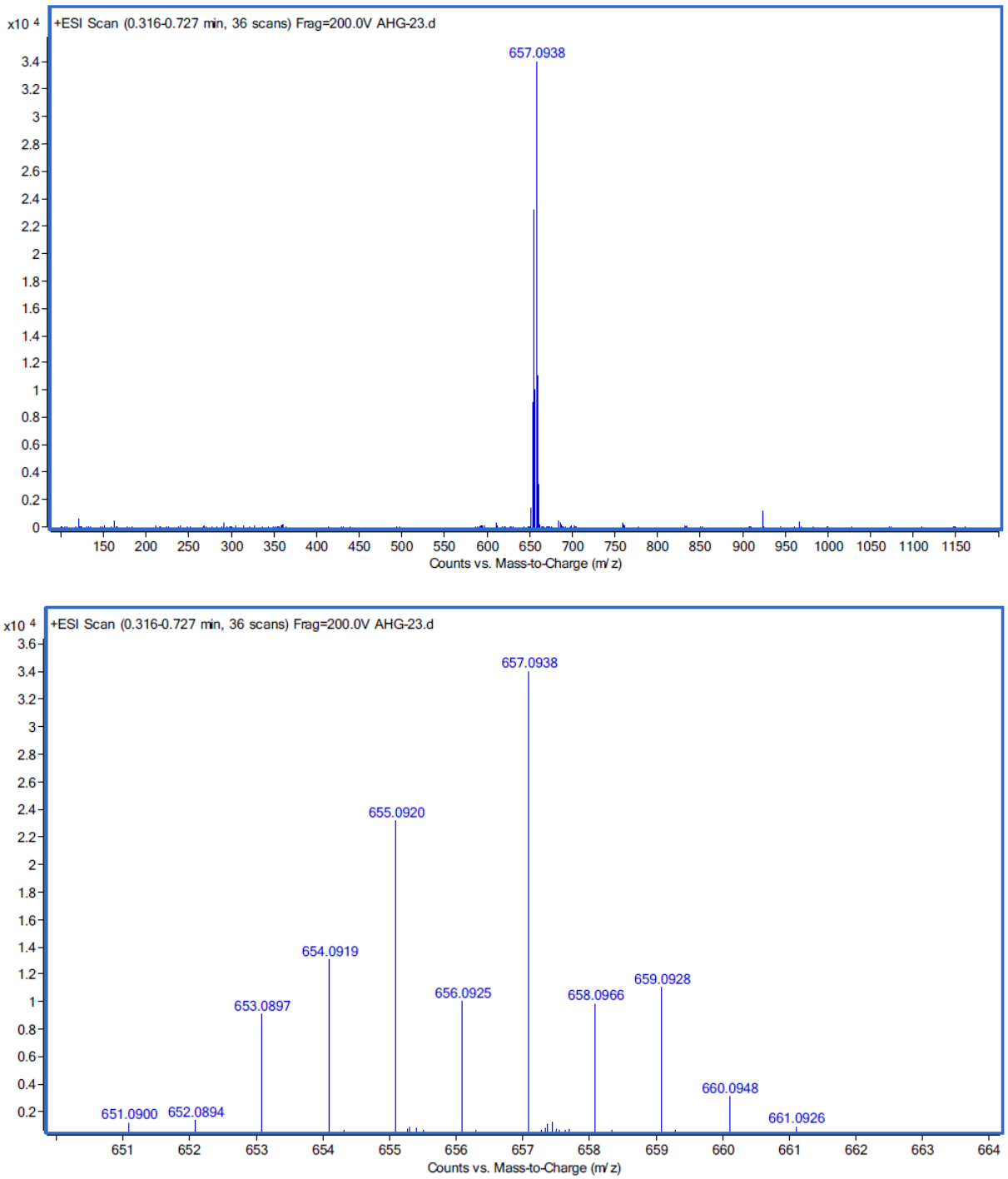

Figure S18. ESI-HRMS spectrum of complex **Os2** (positive detection mode).

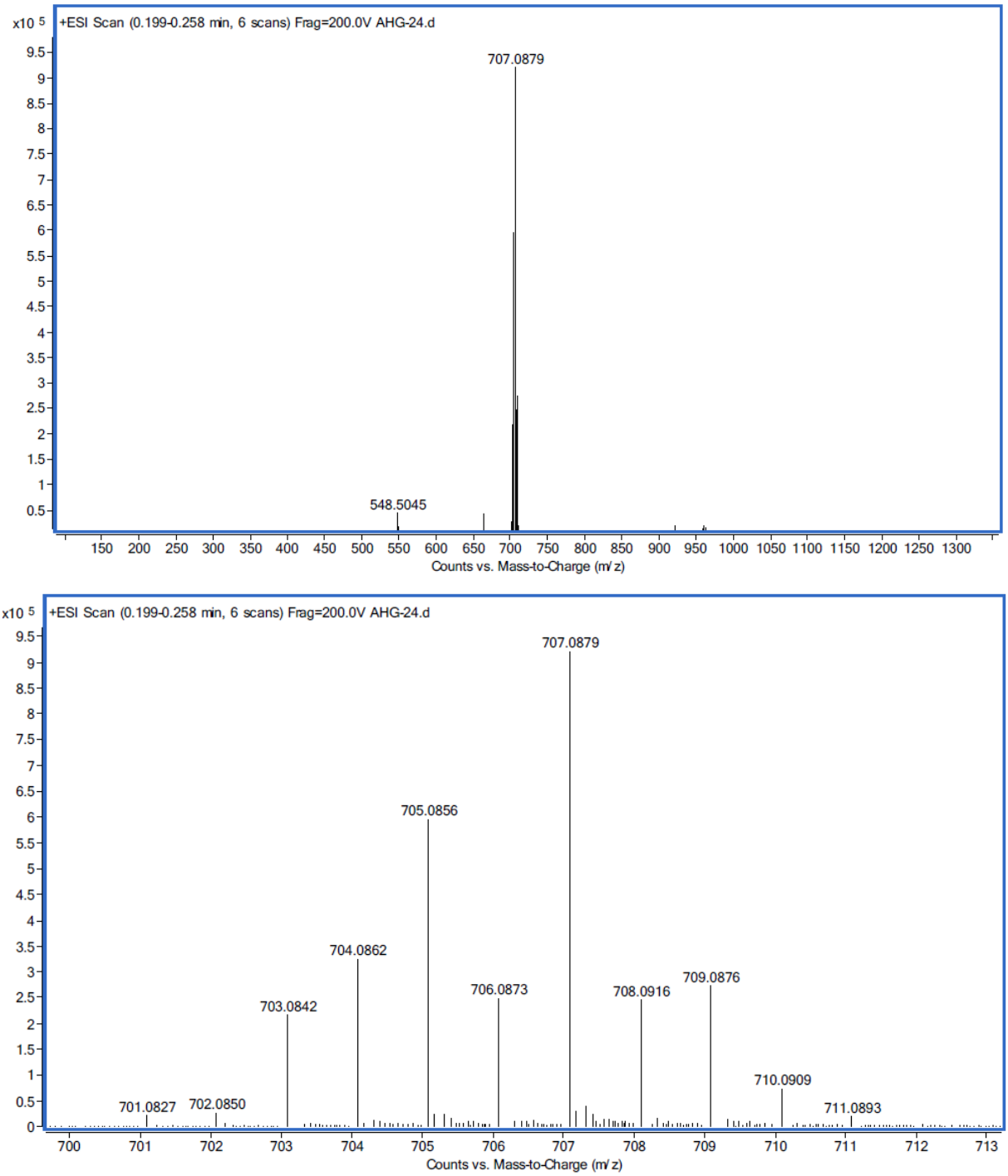

Figure S19. ESI-HRMS spectrum of complex **Os3** (positive detection mode).

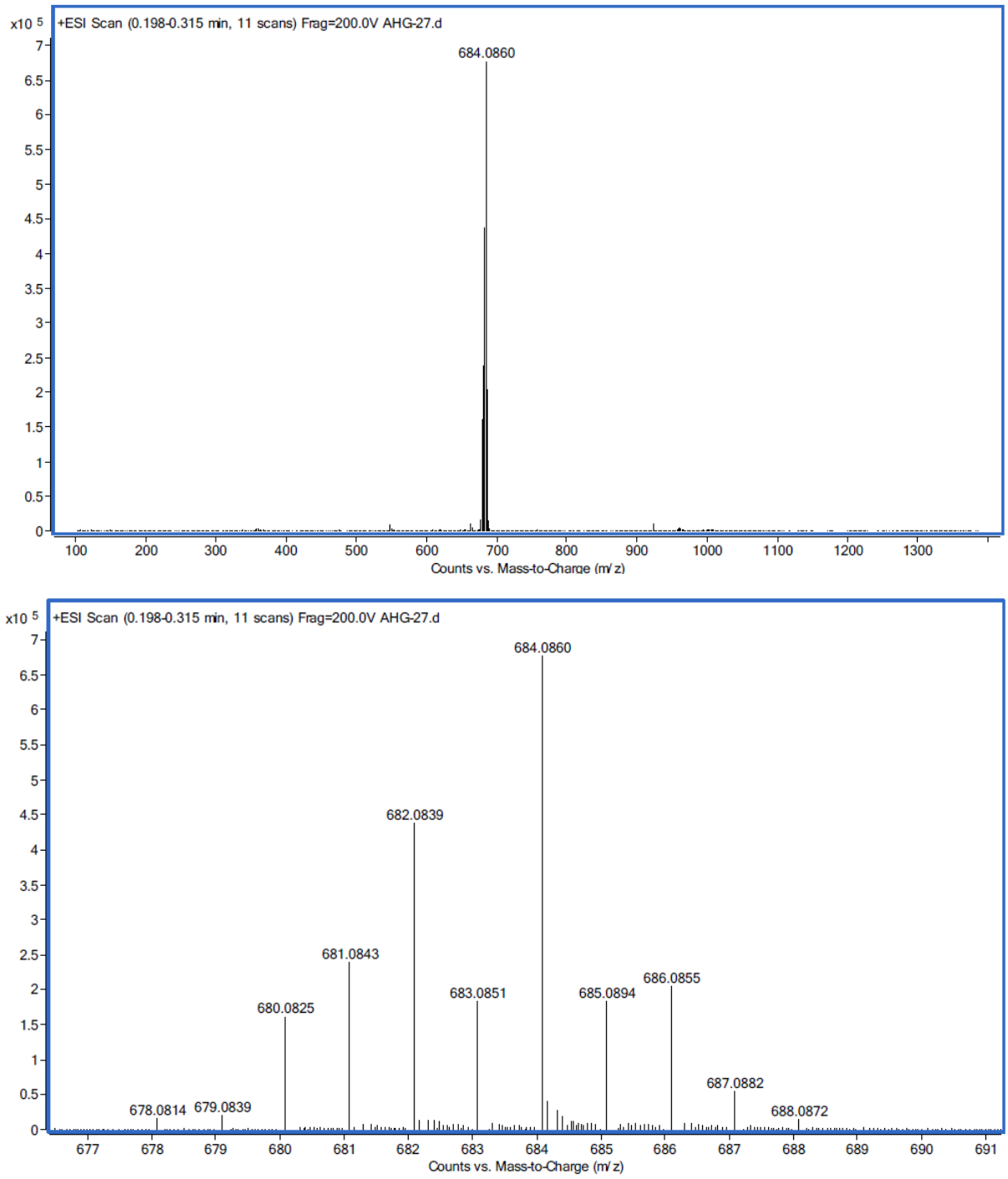

Figure S20. ESI-HRMS spectrum of complex **Os4** (positive detection mode).

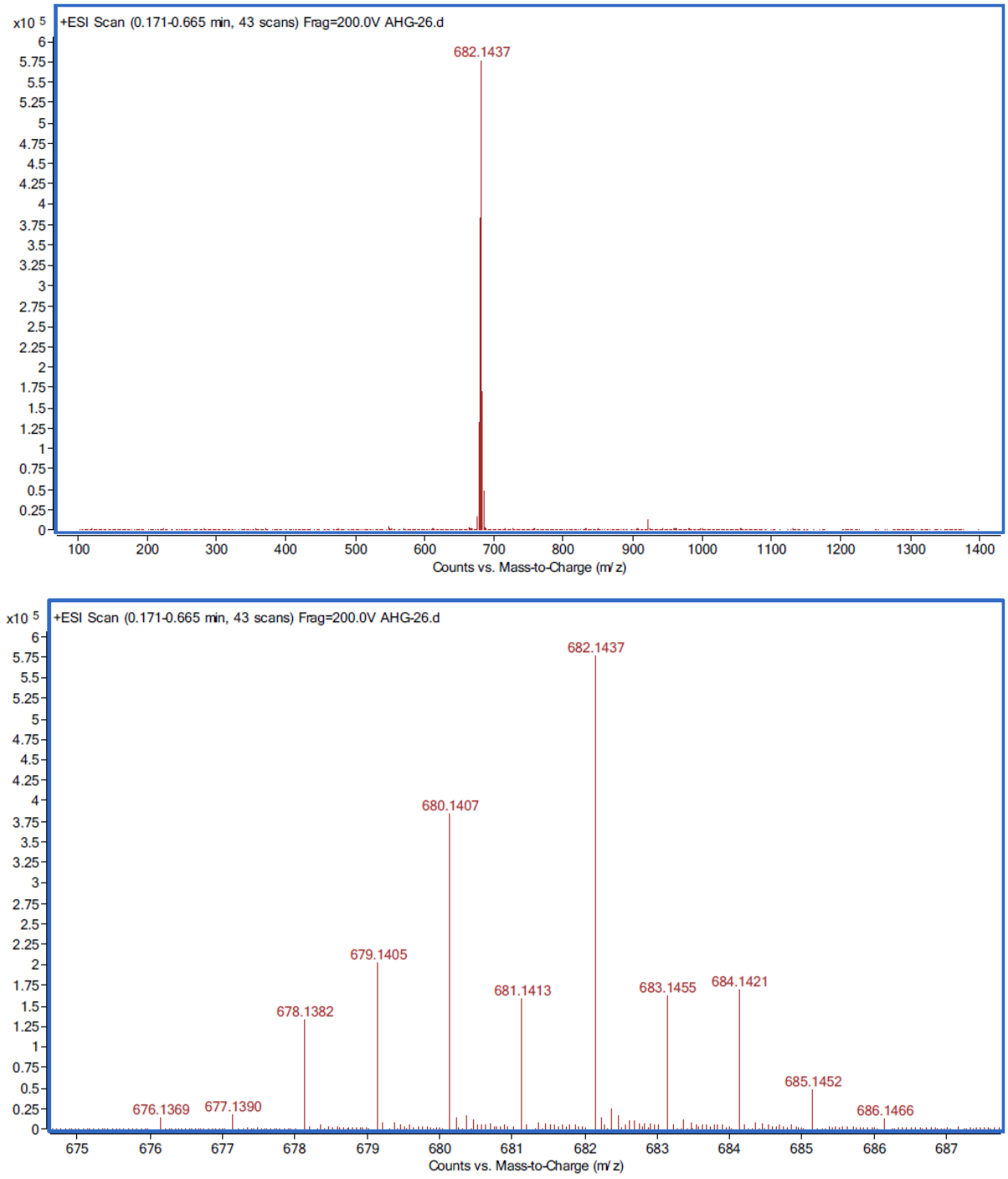

Figure S21. ESI-HRMS spectrum of complex **Os5** (positive detection mode).

4. High performance liquid chromatography (HPLC) analysis

Table S1. HPLC method

Time (min)	0.1 % formic acid in H_2O	0.1 % formic acid in CH_3CN	Flow (mL/min)
0	80	20	0.4
25	0	100	

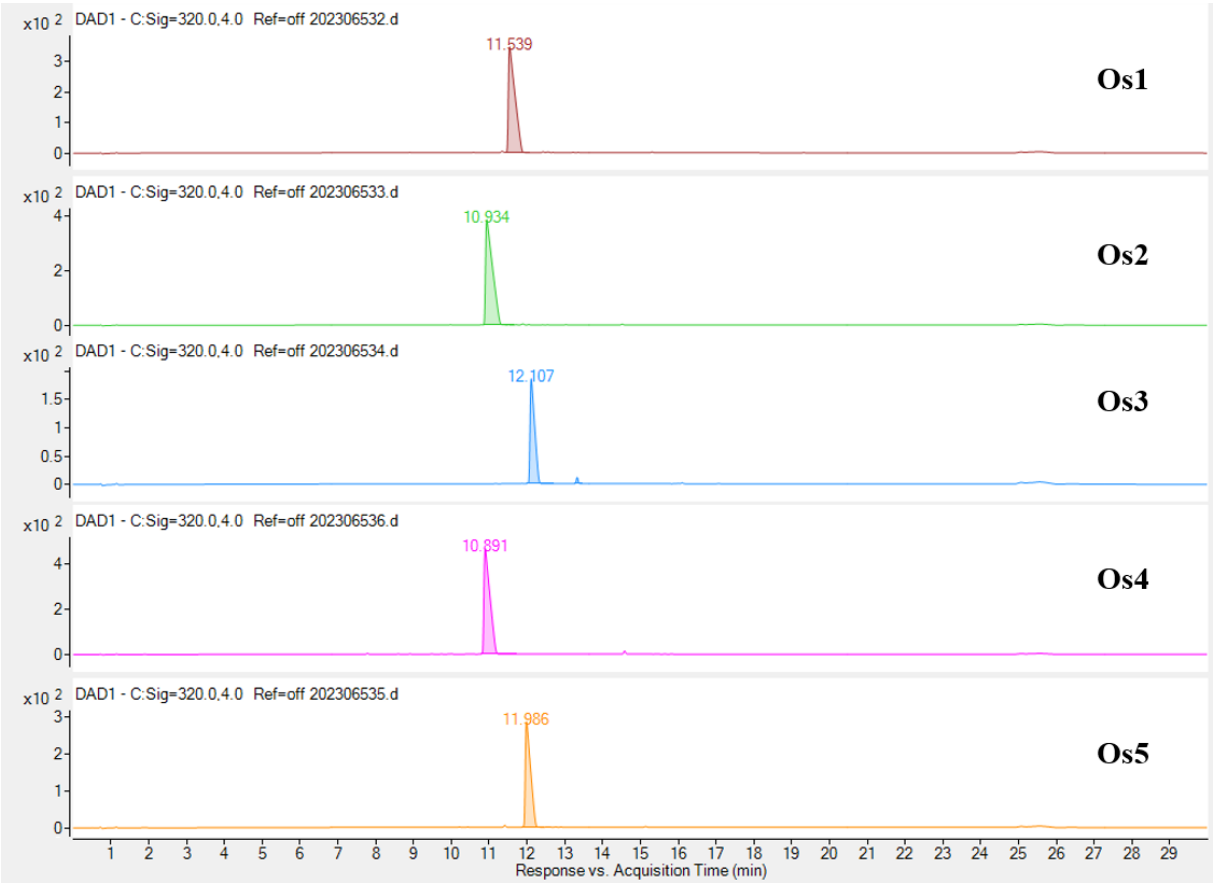

Figure S22. HPLC chromatograms with UV detection at 420 nm of complexes **Os1-Os5**.

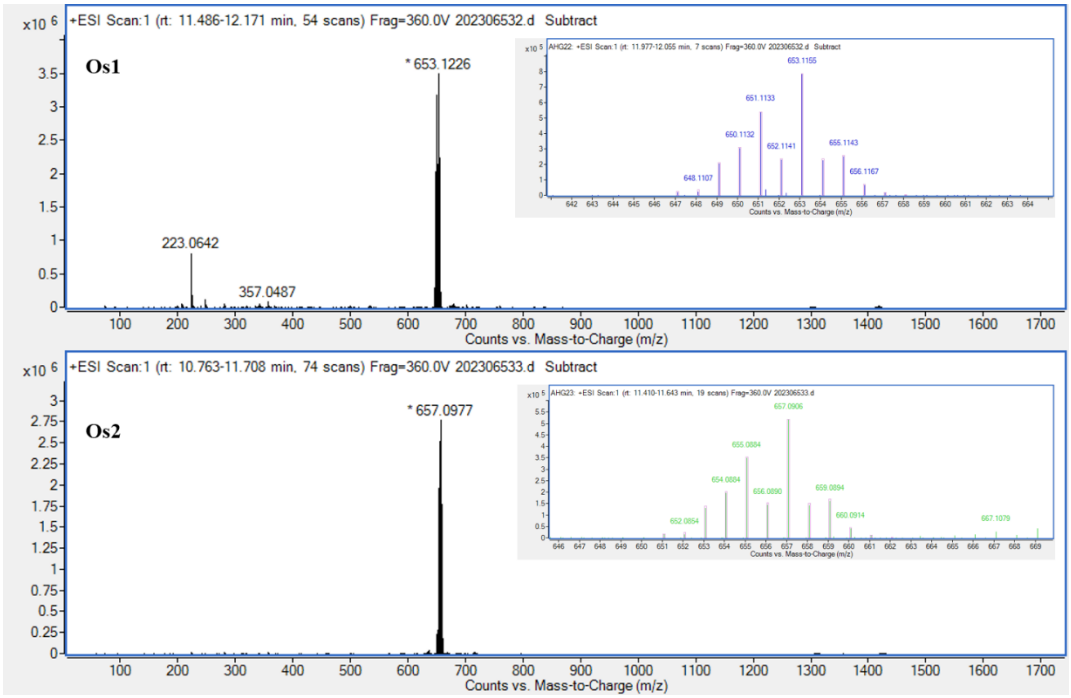

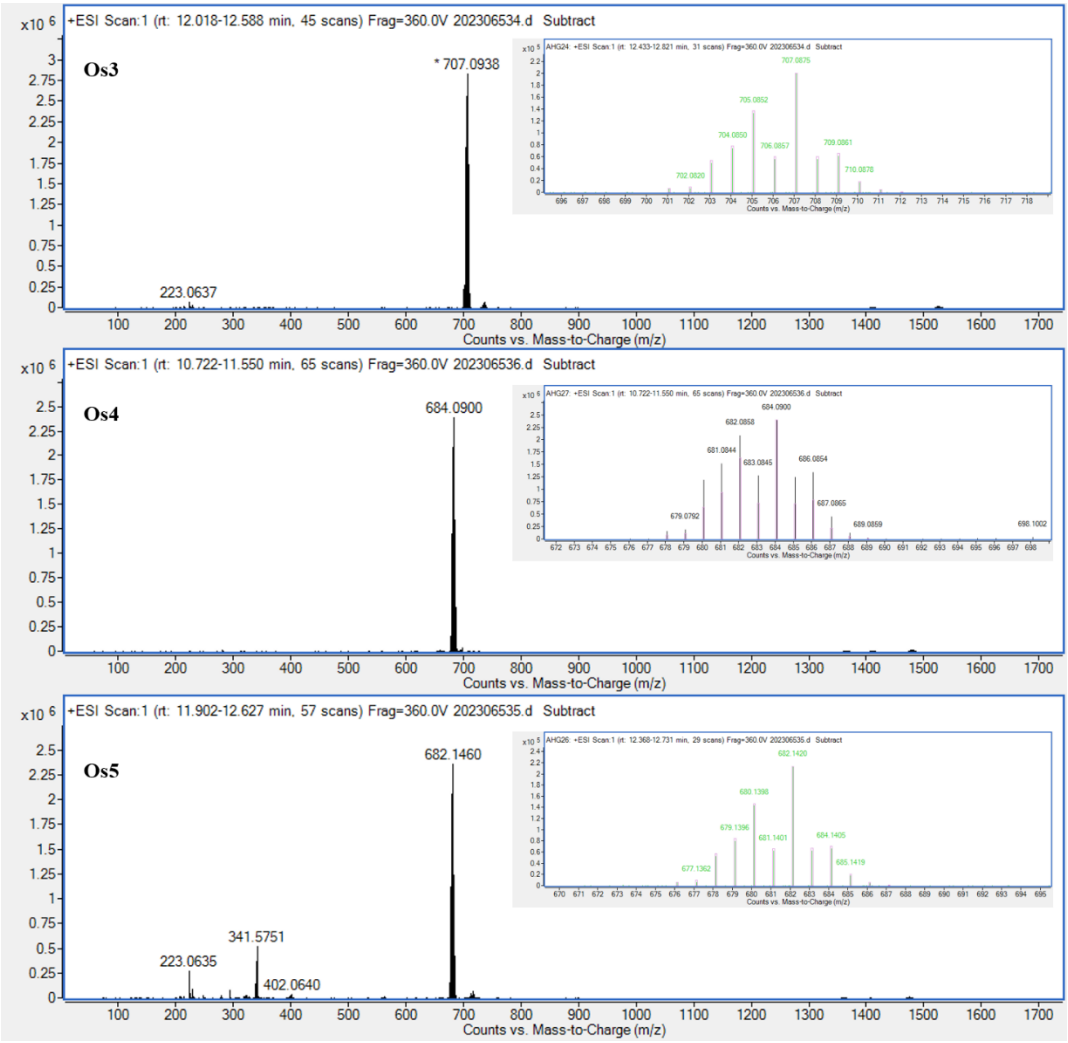

Figure S23. Mass spectra of the 11-12 min peak of chromatograms of Figure S22 with peak of interest extracted for all complexes.

5. X-Ray diffraction

Table S2. X-ray diffraction data of complex **Os3**

Empirical formula	**$C_{26}H_{23}ClF_9N_4OsPS$**	
Formula weight	851.16	
Temperature	100(2) K	
Wavelength	0,71073 Å	
Crystal system	Orthorhombic	
Space group	Pbcn	
Unit cell dimensions	a = 26.697(4) Å	a= 90°
	b = 9.8177(15) Å	b= 90°
	c = 21.815(3) Å	g = 90°

Volume	5717.9(14) $Å^3$
Z	8
Density (calculated)	1.978 Mg/m^3
Absorption coefficient	4.768 mm^{-1}
F(000)	3296
Crystal size	0.320 x 0.170 x 0.150 mm^3
Theta range for data collection	2.017 to 26.371°
Index ranges	-33≤ h≤ 33, -12≤ k≤ 12, -27≤ l≤ 27
Reflections collected	183983
Independent reflections	5846 [R(int) = 0.0589]
Completeness to theta = 25.242°	100.0 %
Absorption correction	Semi-empirical from equivalents
Max. And min. transmission	0.7461 and 0.5121
Refinement method	Full-matrix least-squares F^2
Data / restraints / parameters	5846 / 58 / 422
Goodness-of-fit on F^2	1.069
Final R indices [I>2sigma(I)]	R1 = 0.0186, wR2 = 0.0411
R indices (all data)	R1 = 0.0214, wR2 = 0.0422
Largest diff. Peak and hole	2.033 and -0.616 $e.Å^{-3}$

Table S3. Hydrogen bonds for **Os3** [Å and °]

D-H...A	d(D-H)	d(H...A)	d(D...A)	<(DHA)
C(19)-H(19)...F(33)#1	0.95	2.36	3.004(3)	124.5
C(19)-H(19)...F(35)#1	0.95	2.43	3.358(3)	164.4

Symmetry transformations used to generate equivalent atoms:

#1 -x+1,-y+2,-z+1

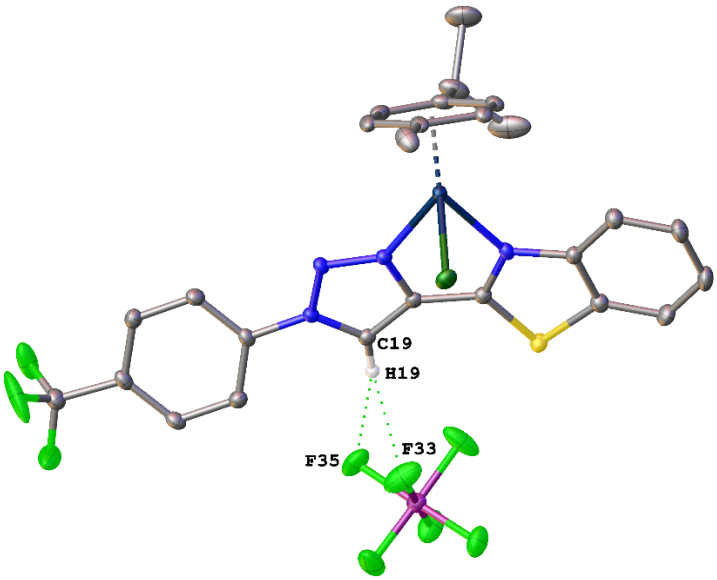

Figure S24. Hydrogen bonds in the structure of **Os3**. Ellipsoids have been represented at 50 % probability

Table S4. Geometrical parameters of the CH···π interactions for **Os3**.

	C-H···centroid ring distance (Å)	C-H···centroid ring angle (º)
C(9)-H(9B)···Plane 1	2,98	139

Plane 1 (S1, C16, C11, N1, C17).

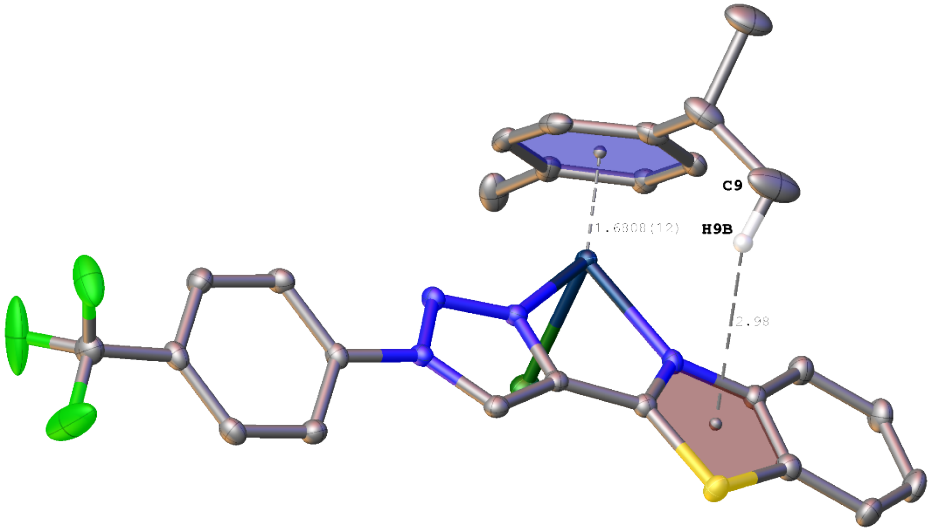

Figure S25. Intermolecular CH-π interactions of **Os3**

Table S5. X-ray diffraction data of complex **Os5**

Empirical formula	**$C_{27}H_{29}ClF_6N_5OsPS$**
Formula weight	826.23
Temperature	100(2) K
Wavelength	0,71073 Å
Crystal system	Orthorhombic
Space group	Pccn
Unit cell dimensions	a = 25.037(2) Å α =90°
	b = 10.6927(11) Å β =90°
	c = 21.7489(18) Å γ =90°
Volume	5822.4(9) $Å^3$
Z	8
Density (calculated)	1.885 Mg/m^3
Absorption coefficient	4.666 mm^{-1}
F(000)	3232
Crystal size	0.240 x 0.200 x 0.120 mm^3
Theta range for data collection	1.873 to 30.523°.
Index ranges	$-35 \leq h \leq 35$, $-15 \leq k \leq 15$, $-30 \leq l \leq 31$
Reflections collected	139131
Independent reflections	8896 [R(int) = 0.0871]
Completeness to theta = 25.242°	100.0 %
Absorption correction	Semi-empirical from equivalents
Max. And min. transmission	0.7461 and 0.5537
Refinement method	Full-matrix least-squares F^2
Data / restraints / parameters	8896 / 0 / 384
Goodness-of-fit on F^2	1.043
Final R indices [I>2sigma(I)]	C
R indices (all data)	R1 = 0.0392, wR2 = 0.0528
Largest diff. Peak and hole	0.767 and -0.837 $e.Å^{-3}$

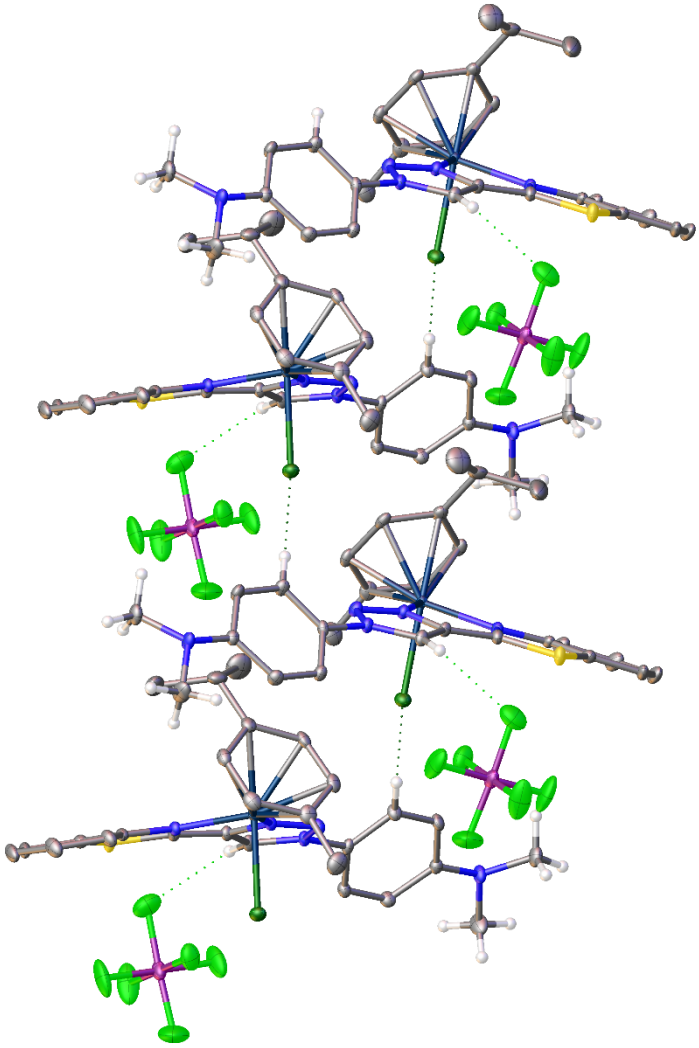

Figure S26. Hydrogen bonds in the structure of **Os5**. Ellipsoids have been represented at 50 % probability

Table S6. Hydrogen bonds for **Os5** [Å and °]

D-H...A	d(D-H)	d(H...A)	d(D...A)	<(DHA)
C(19)-H(19)...F(6)#1	0.95	2.44	3.176(3)	134.7
C(25)-H(25)...Cl(1)#2	0.95	2.73	3.683(3)	177.3
C(26)-H(26C)...F(3)#3	0.98	2.53	3.132(4)	119.8
C(27)-H(27C)...F(6)#4	0.98	2.49	3.316(3)	141.2

Symmetry transformations used to generate equivalent atoms:

#1 -x+3/2, -y+3/2,z; #2 -x+1,y-1/2,-z+3/2; #3 x-1/2,y+1/2,-z+1; #4 x-1/2,y-1/2,-z+1

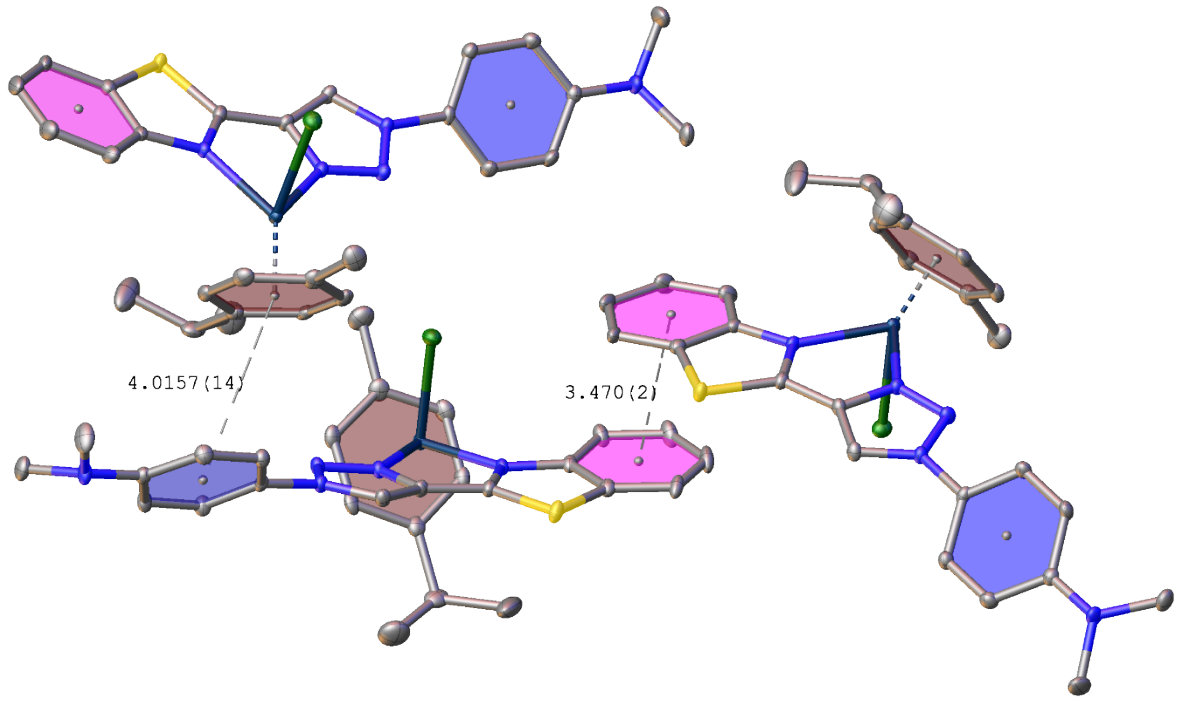

Figure S27. Intermolecular π-π interactions of **Os5**.

Table S7. Geometrical parameters of the π···π stacking interactions for **Os5.**

π···π interaction	centroid-centroid distance	Plane-Plane angle (º)	θ
Plane 1- Plane 1	3.470(2)	1,60(12)	0,743
Plane 2- Plane 3	4.0157(14)	11,57(8)	2.304)/1.597(4)

Plane 1 (C11, C12, C13, C14, C15 y C16), Plane 2 (C1, C2, C3, C4, C5 y C6) and Plane 3 (C20, C21, C22, C23, C24 y C25).

Table S8. Geometrical parameters of the CH···π interactions for **Os5**.

	C-H···centroid ring distance (Å)	C-H···centroid ring angle (º)
C(9)-H(9A)···Plane 1	2.95	137
C(9)-H(9C)···Plane 4	2.94	164

Plane 1 (C11, C12, C13, C14, C15 y C16) and Plane 4 (S6, C16, C11, N1, C17)

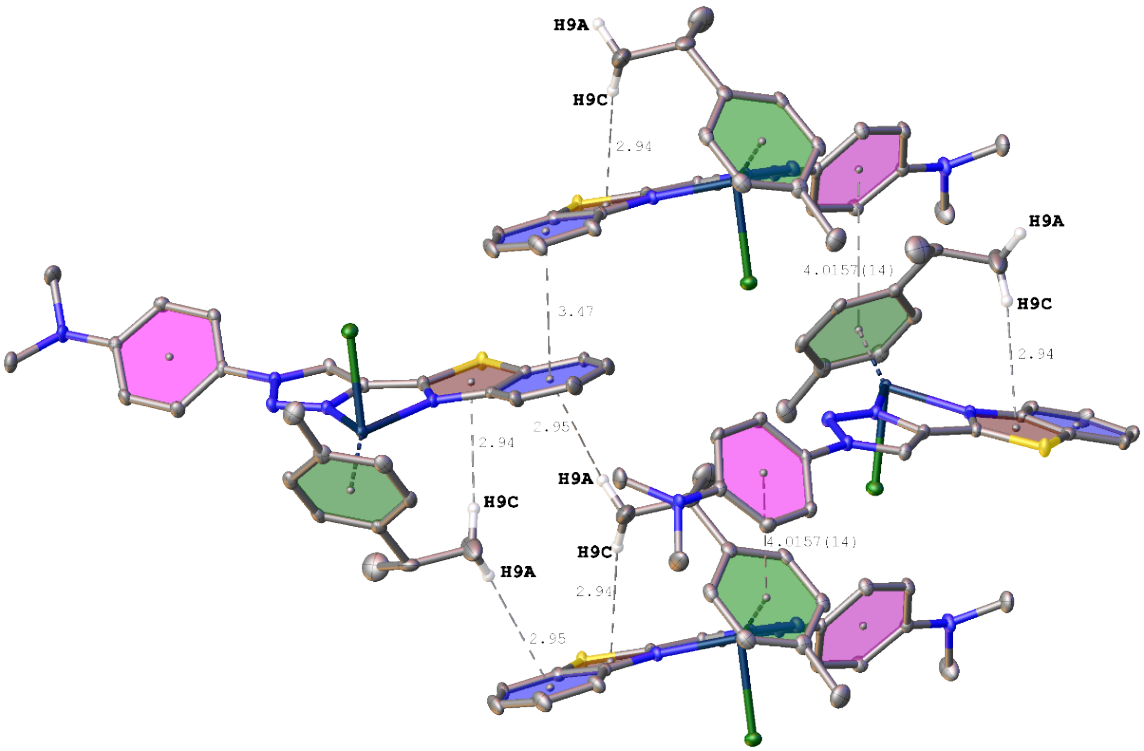

Figure S28. Intermolecular π-π and CH-π interactions of **Ir3**

6. Photophysical properties

Table S9. Absorption wavelengths (λ_{abs}) and molar extinction coefficient (ε) of complexes in areated acetonitrile and DMSO, and excitation wavelengths (λ_{ex}) and emission wavelengths (λ_{em}) in DMSO.

Comp.	Solvent	λ (nm) (ε, $M^{-1}cm^{-1}$)	λ_{ex} (nm)	λ_{em} (nm)
Os1	CH_3CN	253 (19724) 311 (22952) 379h (4298)	-	-
	DMSO	260 (19016) 314 (22810) 377h (4684)	310	365
Os2	CH_3CN	252 (17458) 312 (19978) 380h (3888)	-	-
	DMSO	260 (17372) 314 (21142) 378h (4558)	310	364
Os3	CH_3CN	251 (18694) 311 (22430) 380h (5114)	-	-
	DMSO	260 (15486) 315 (20336) 378h (6406)	310	370
Os4	CH_3CN	259 (16842) 315 (24990) 388h (3556)	-	-
	DMSO	261 (17880) 319 (26686) 382h (6406)	320	412
Os5	CH_3CN	251 (17002) 326 (27296) 360h (21758)	-	-
	DMSO	259 (14012) 328 (26770) 357h (22538)	360	529

7. Stability studies

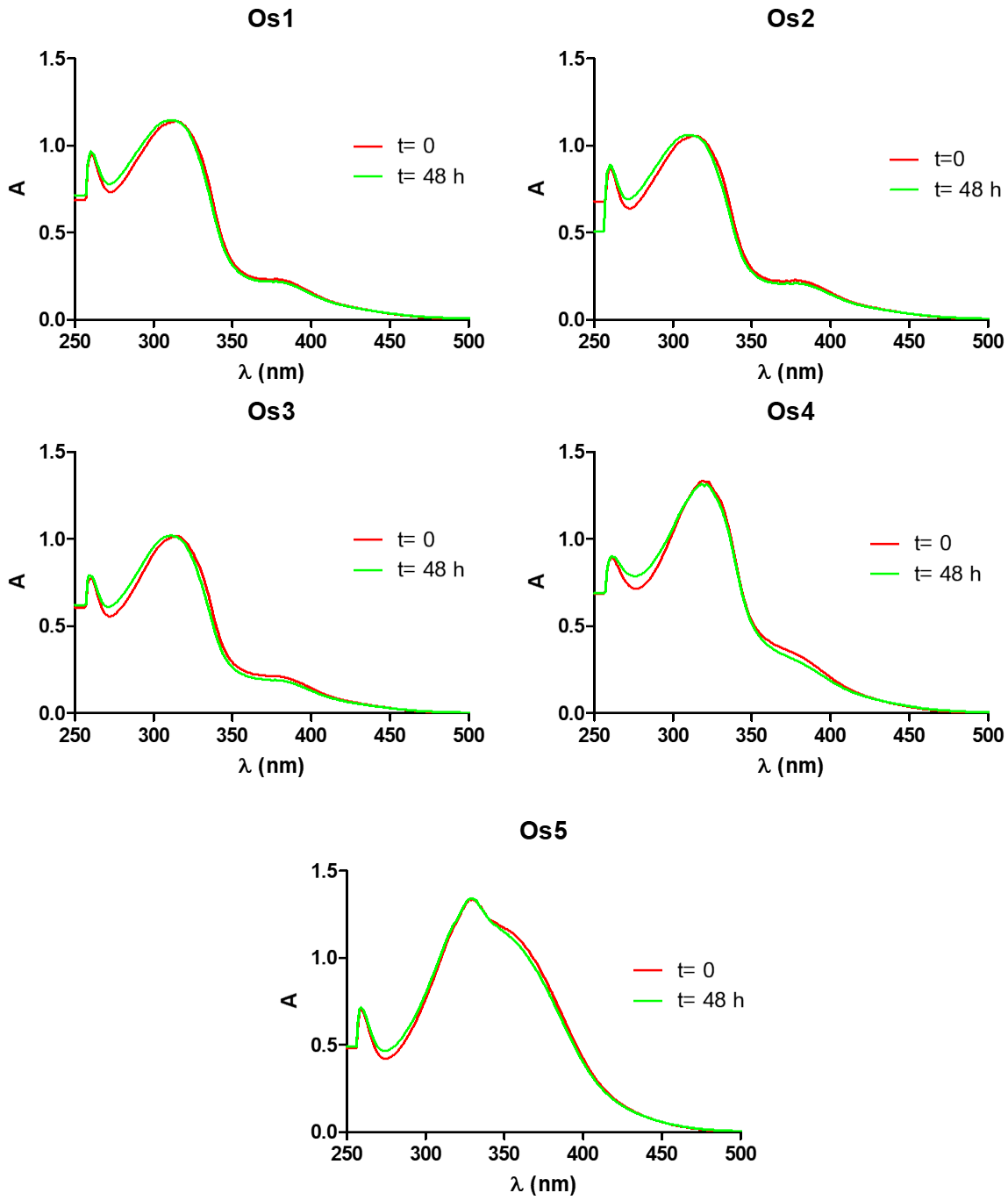

Figure S29. UV-Visible absorption spectra of complexes **Os1-Os5** (50 μM) in DMSO at t=0 anf after 48 h.

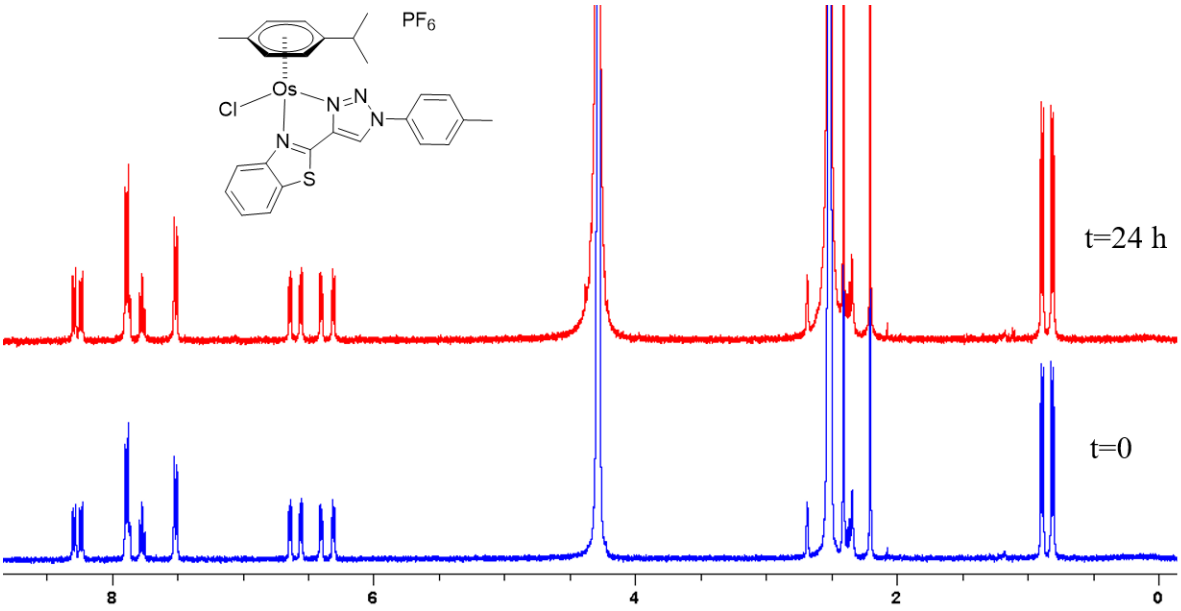

Figure S30. ^{1}H NMR spectra of **Os1** (1mM) in D_2O/DMSO-d_6 (1:2) at t=0 and after 24 h.

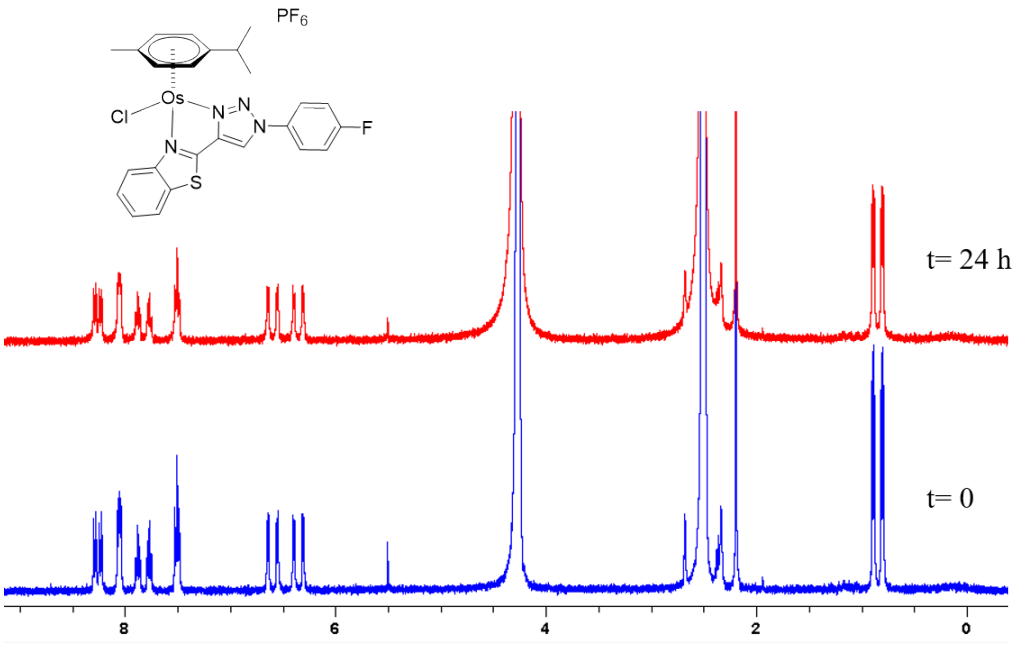

Figure S31. ^{1}H NMR spectra of **Os2** (1mM) in D_2O/DMSO-d_6 (1:2) at t=0 and after 24 h.

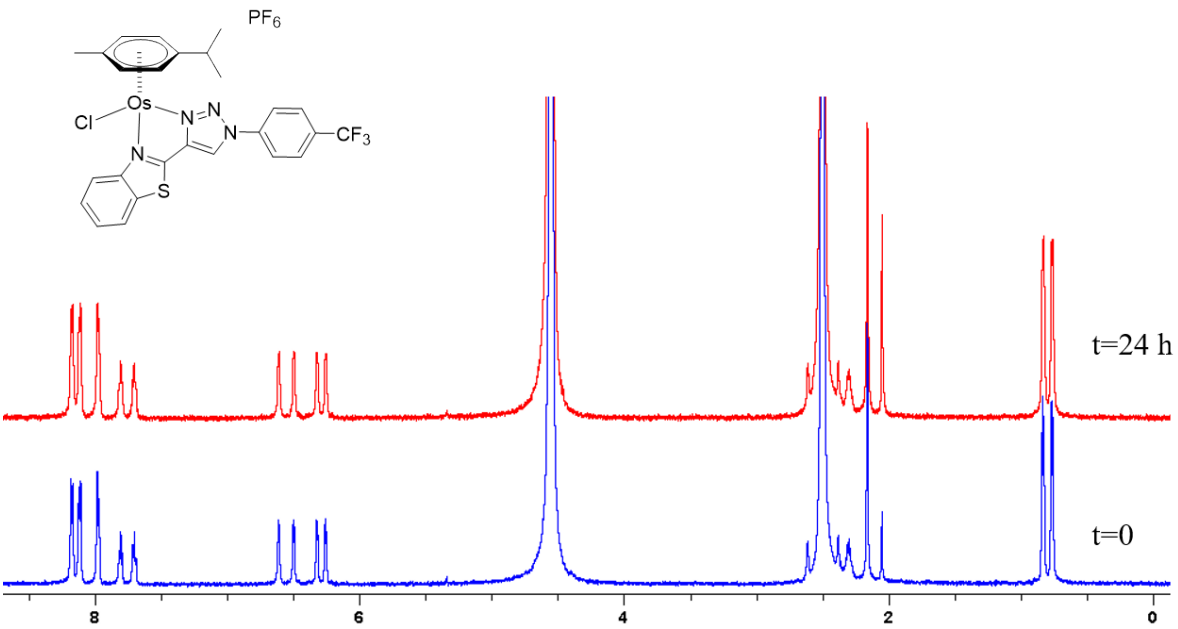

Figure S32. ^{1}H NMR spectra of **Os3** (1mM) in D_2O/DMSO-d_6 (1:2) at t= 0 and after 24 h.

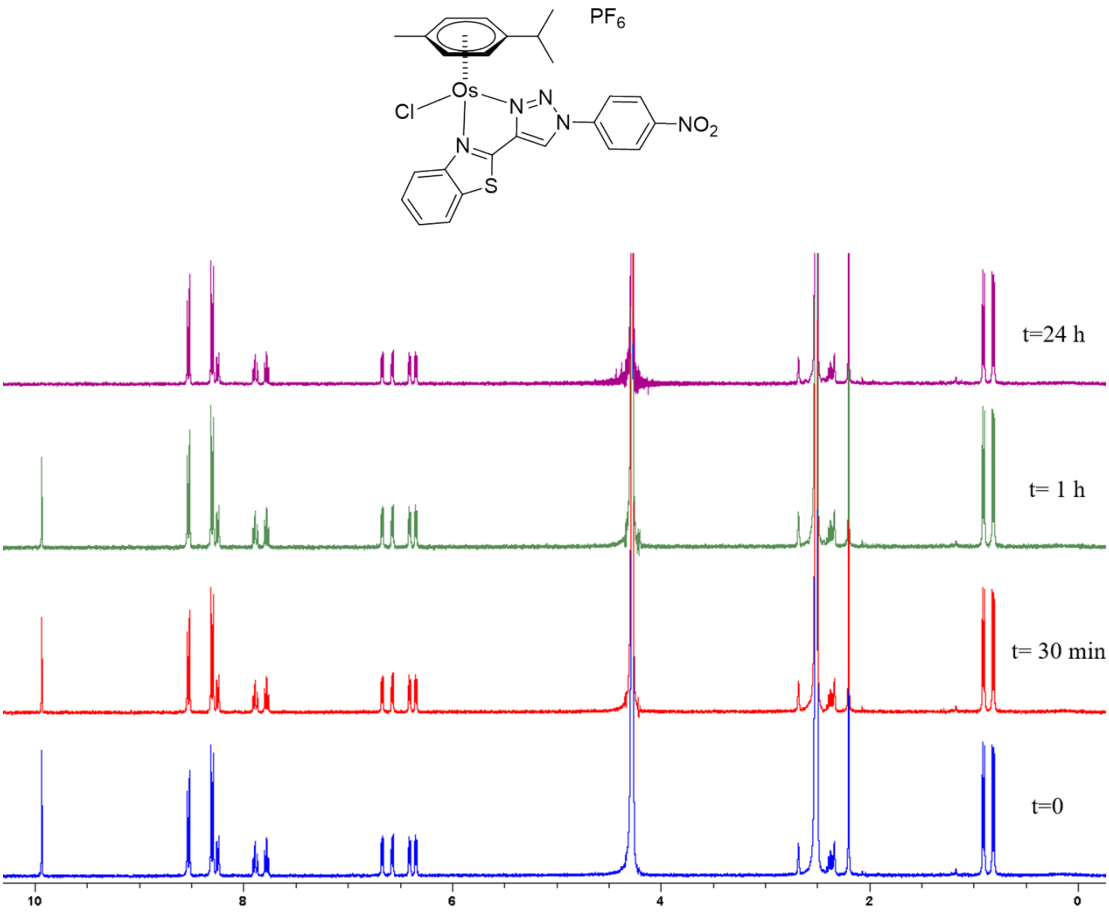

Figure S33. ^{1}H NMR spectra of **Os4** (1mM) in D_2O/DMSO-d_6 (1:2) at different times.

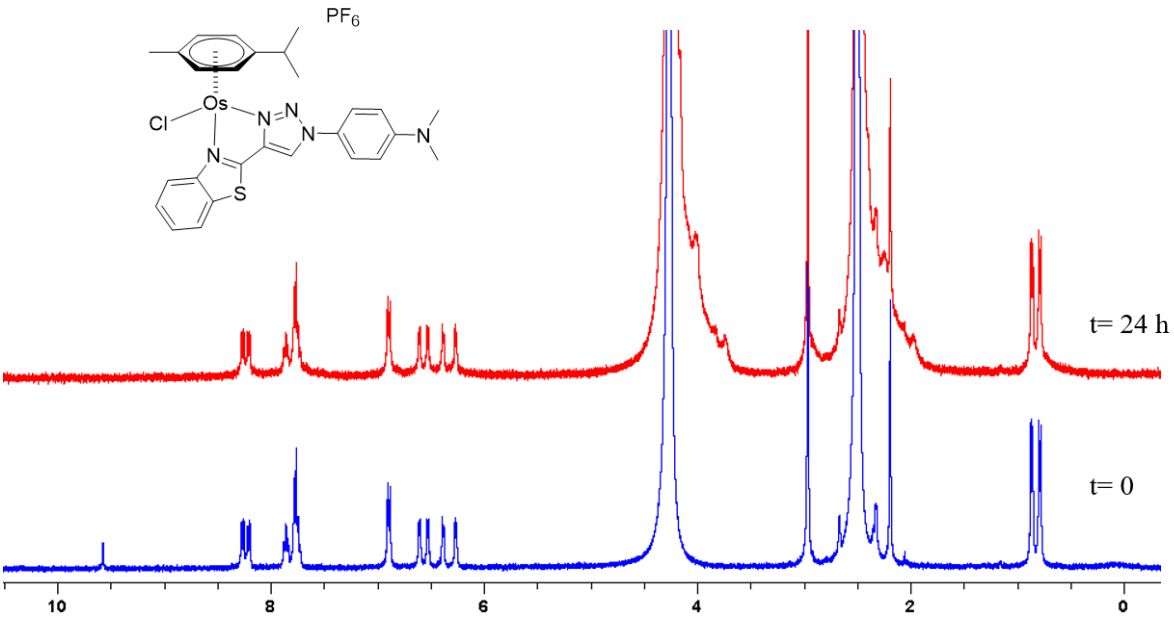

Figure S34. ^{1}H NMR spectra of **Os5** (1mM) in D_2O/DMSO-d_6 (1:2) at t=0 and after 24 h.

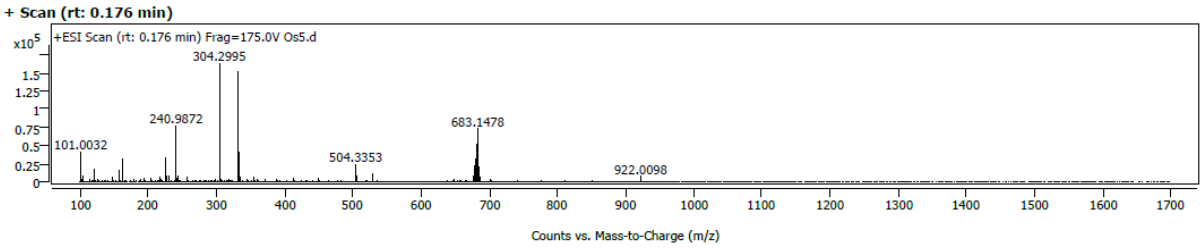

Figure S35. ESI-MS spectra of **Os5** (1mM) in D_2O/DMSO-d_6 (1:2) after 24 h.

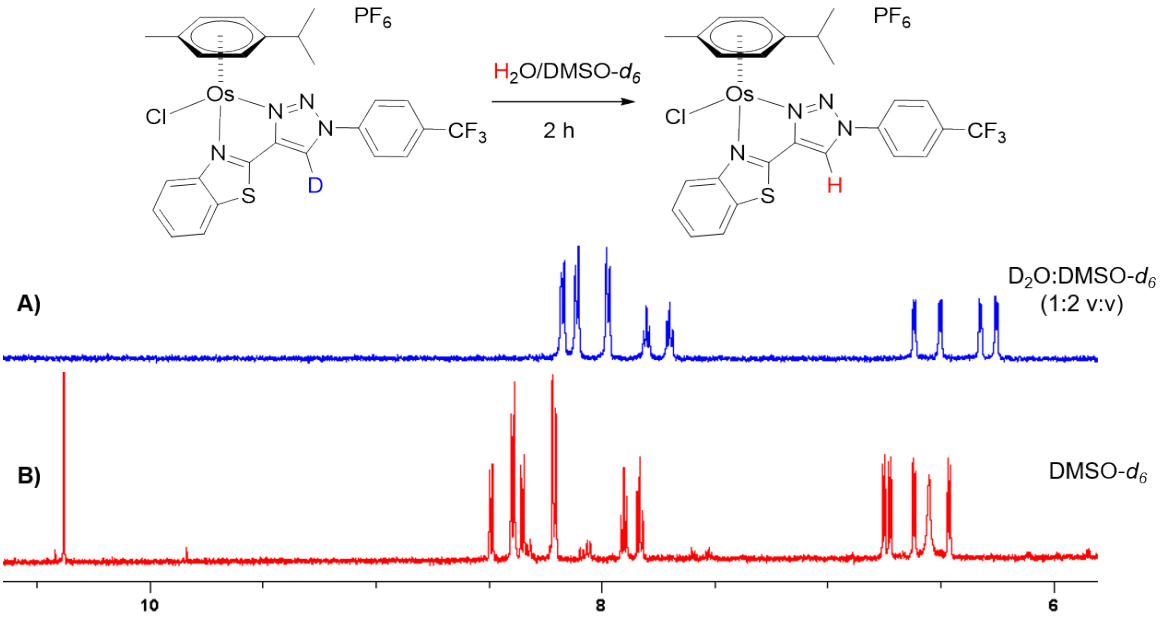

Figure S36. ^{1}H NMR spectra of **Os3** (1mM): **A**) in D_2O:DMSO-d_6 (1:2) after 1 h. **B**) After removing D_2O under reduced pressure, add 400 µL of H_2O mQ and stirring for 1 h. Subsequently, remove the water once more and dissolve in DMSO-*d_6*.

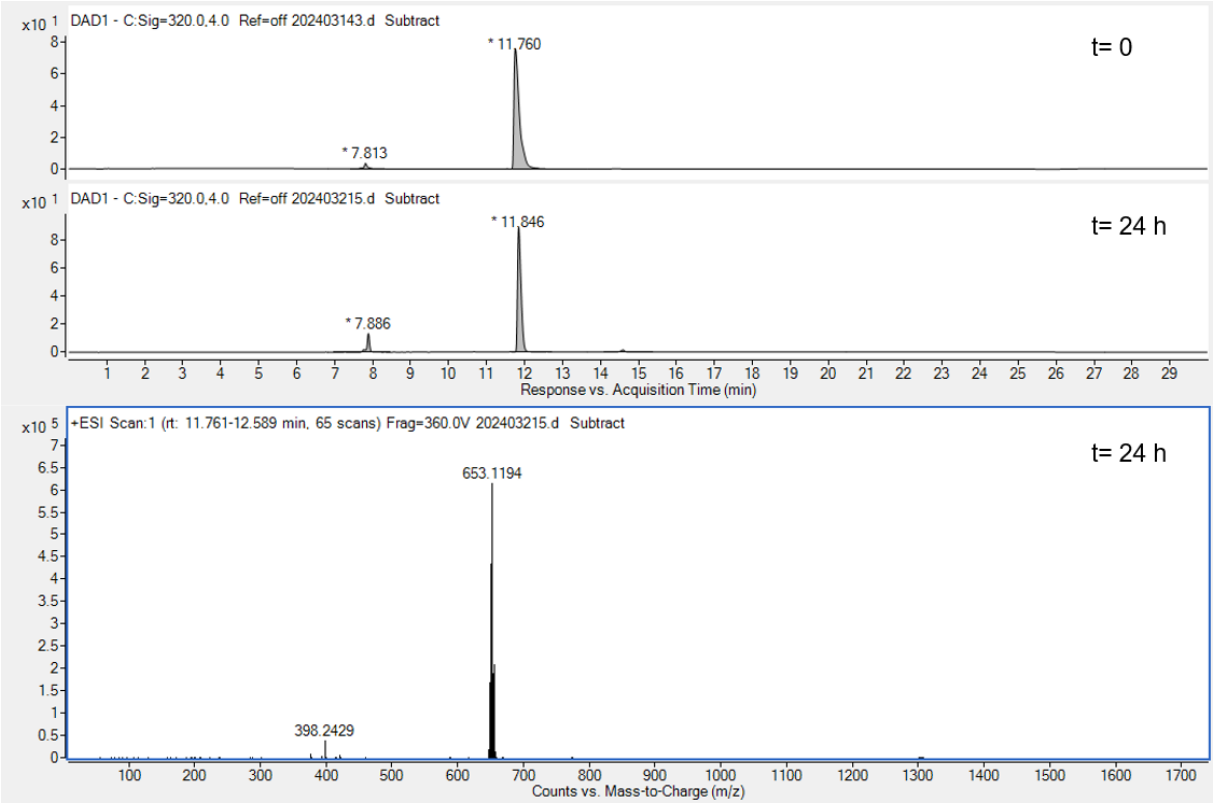

Figure S37. HPLC-MS of **Os1** (10 μM) in water (5 % DMSO) at t=0 and after 24 h at r.t.

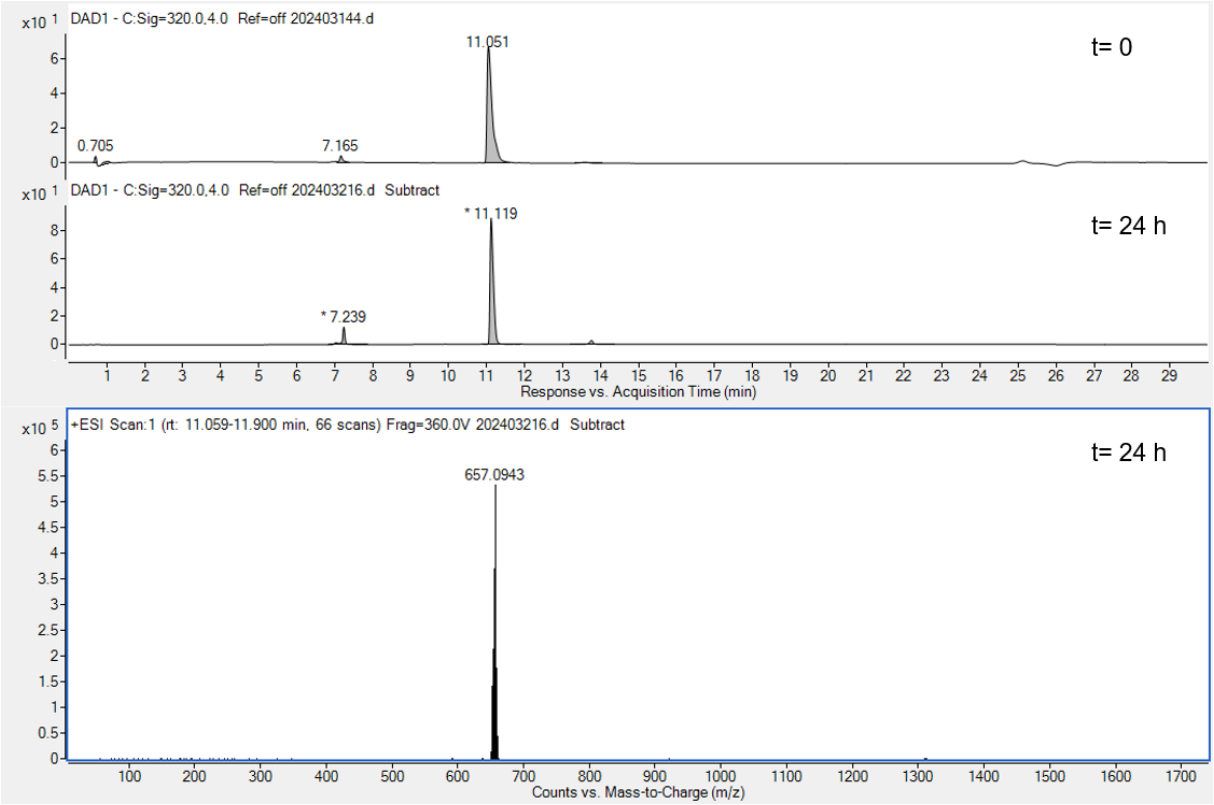

Figure S38. HPLC-MS of **Os2** (10 μM) in water (5 % DMSO) at t=0 and after 24 h at r.t.

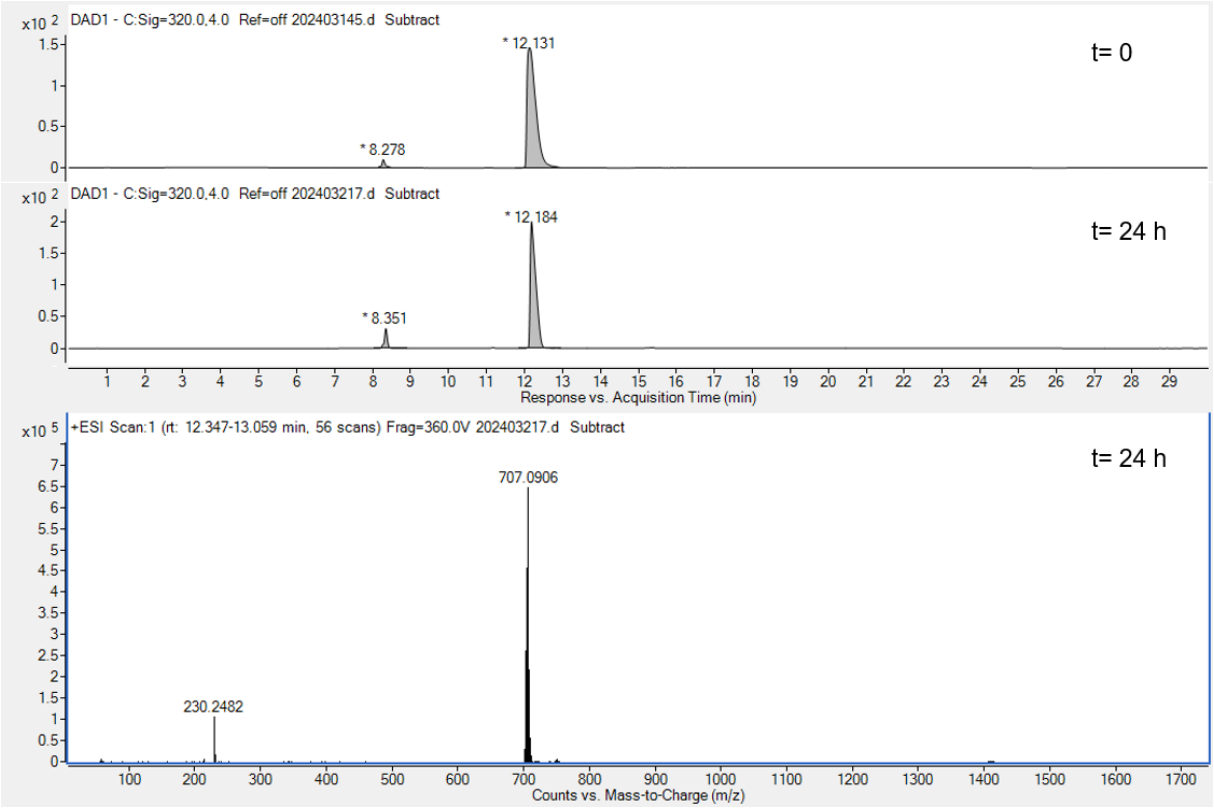

Figure S39. HPLC-MS of **Os3** (10 μM) in water (5 % DMSO) at t=0 and after 24 h at r.t.

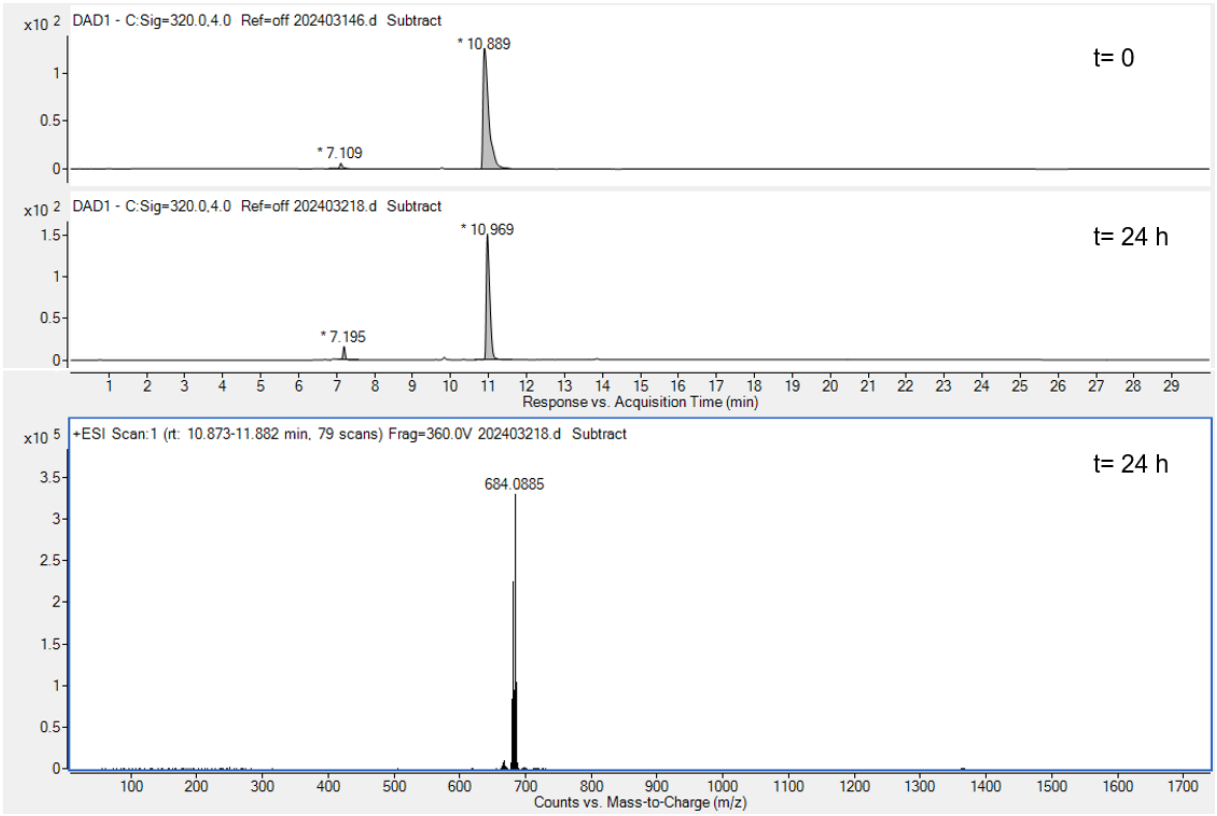

Figure S40. HPLC-MS of **Os4** (10 μM) in water (5 % DMSO) at t=0 and after 24 h at r.t.

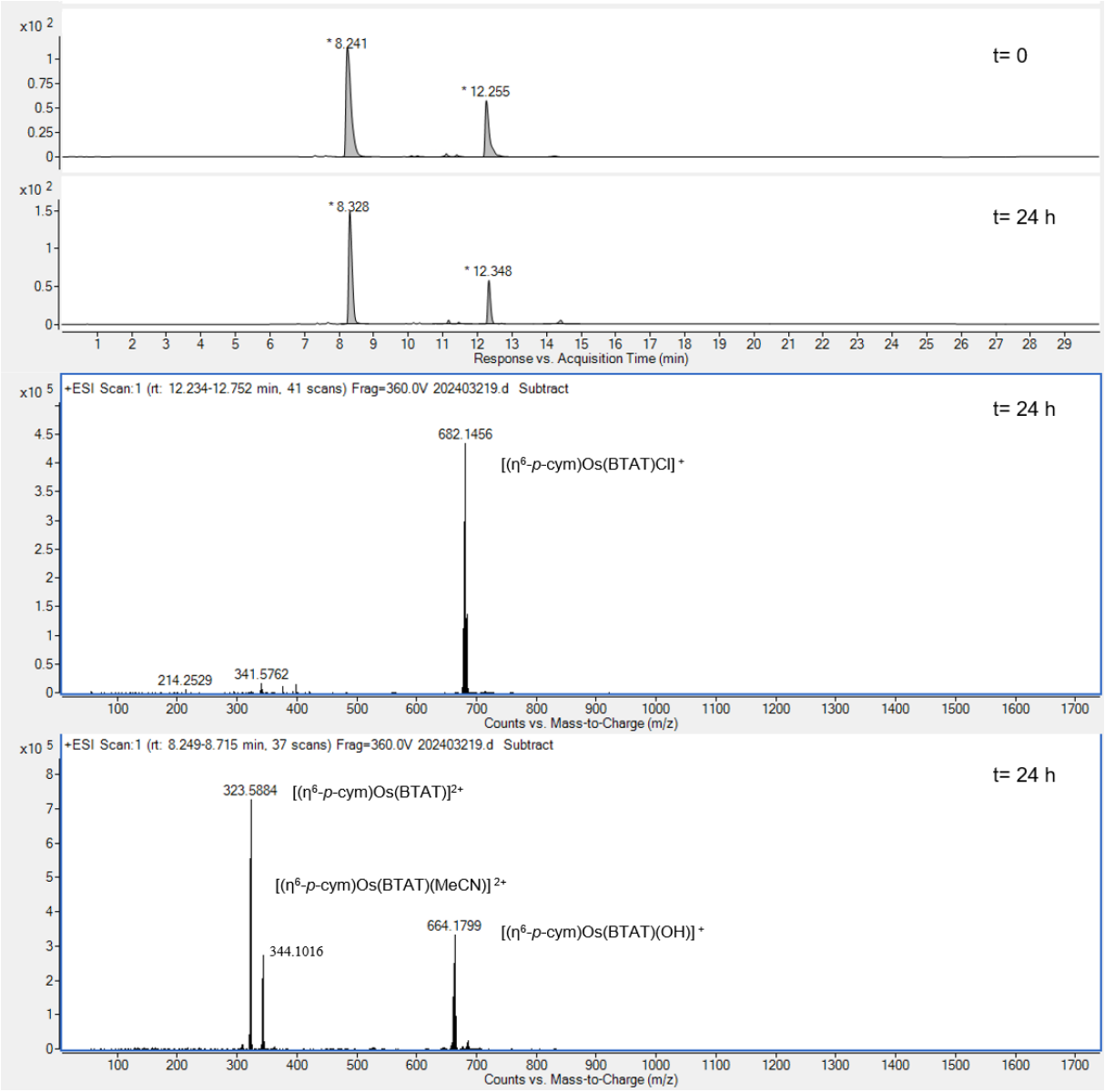

Figure S41. HPLC-MS of **Os5** (10 μM) in water (5 % DMSO) at t=0 and after 24 h at r.t., and mass spectra of the ~12.5 min and ~8.3 min peaks of chromatogram with peaks of interest extracted (see **Table S1** for HPLC method).

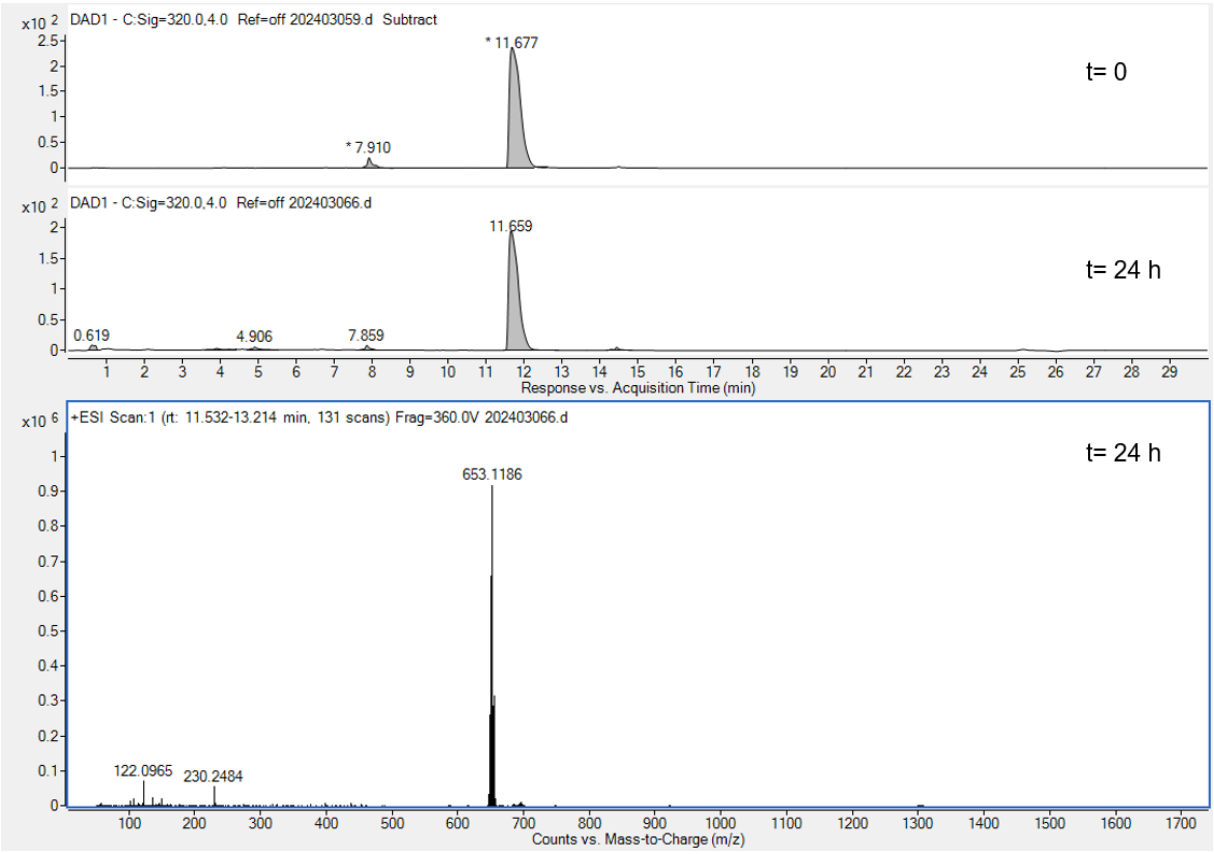

Figure S42. HPLC-MS of **Os1** (10 μM) in RPMI (5 % DMSO) at t=0 and after 24 h at r.t.

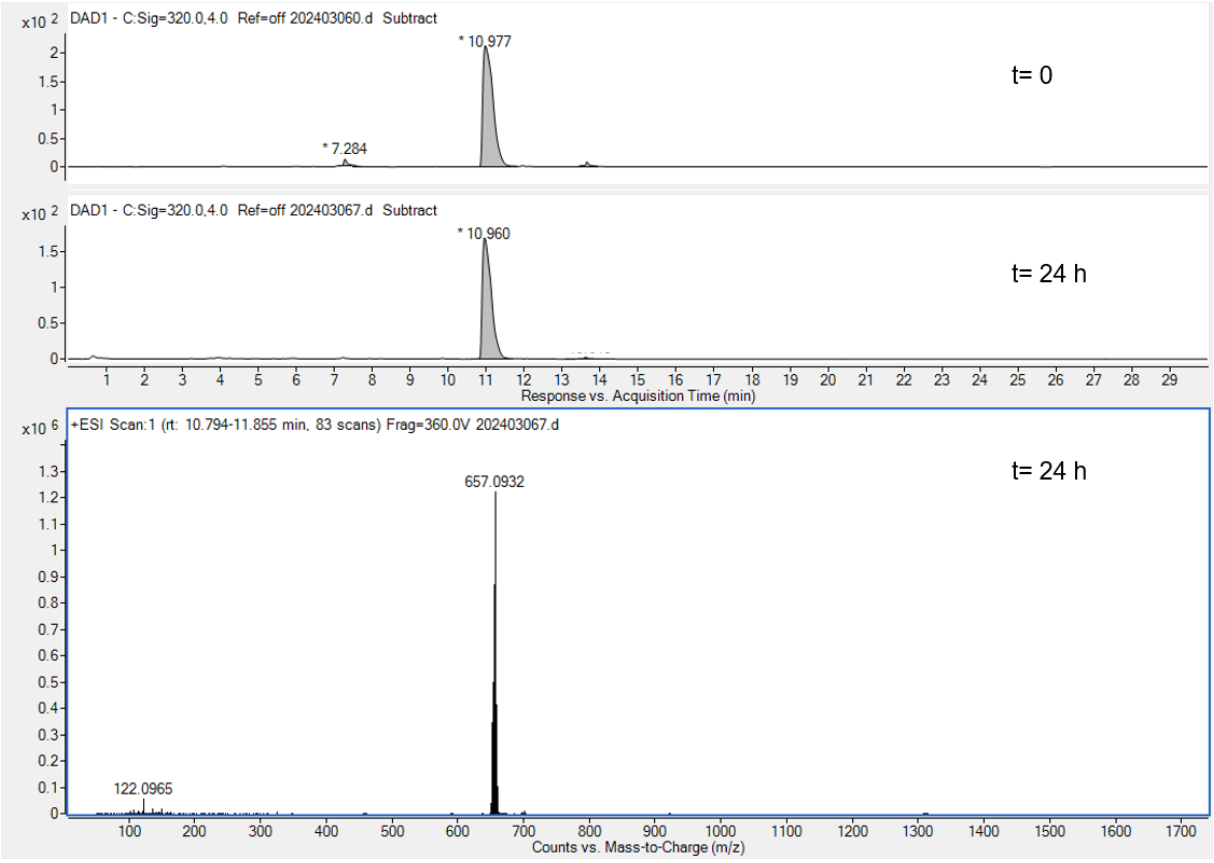

Figure S43. HPLC-MS of **Os2** (10 μM) in RPMI (5 % DMSO) at t=0 and after 24 h at r.t.

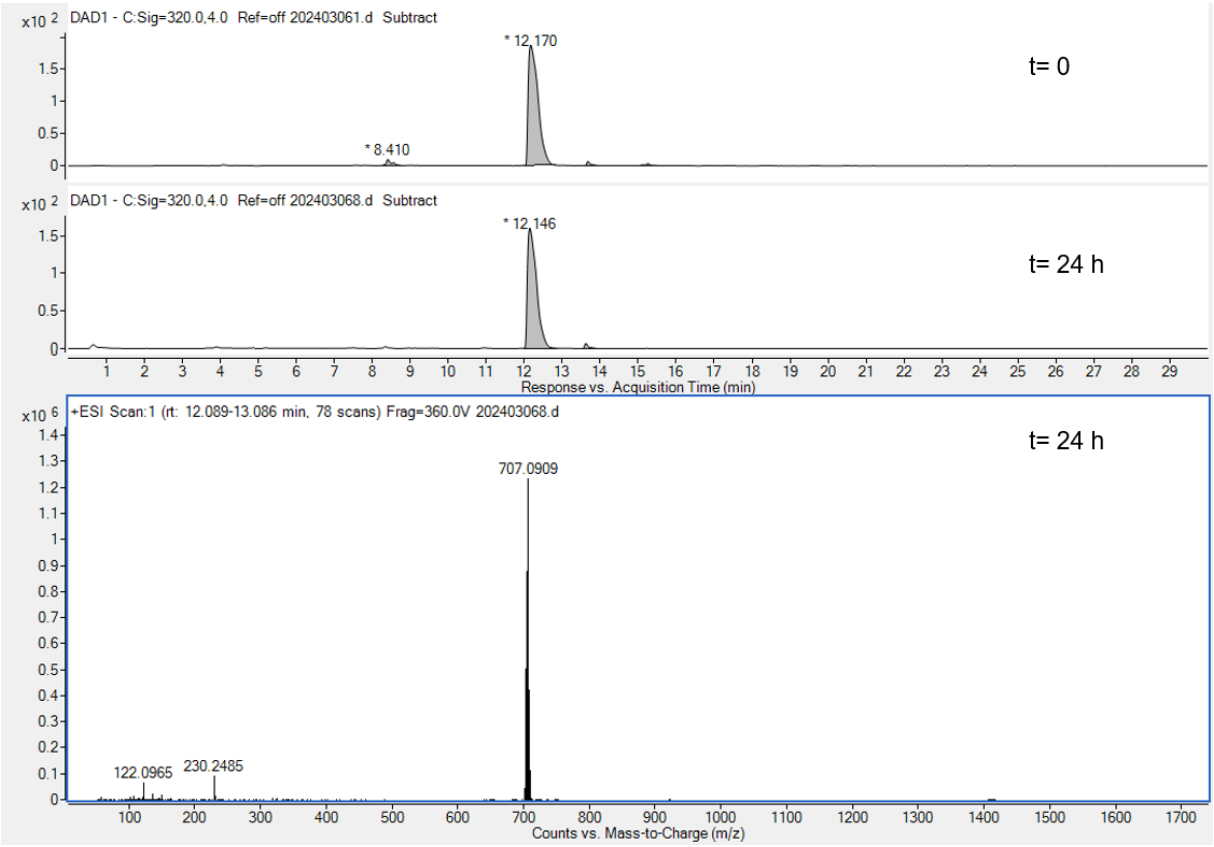

Figure S44. HPLC-MS of **Os3** (10 μM) in RPMI (5 % DMSO) at t=0 and after 24 h at r.t.

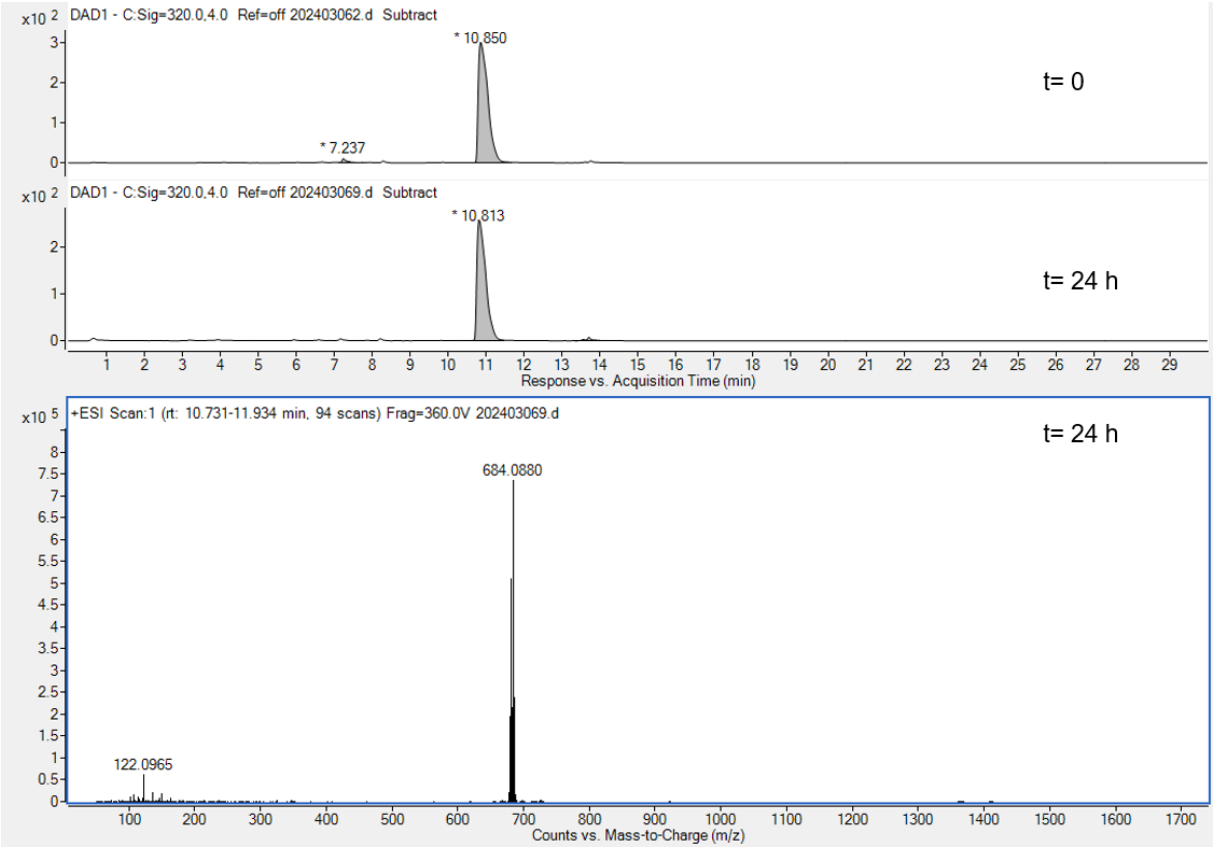

Figure S45. HPLC-MS of **Os4** (10 μM) in RPMI (5 % DMSO) at t=0 and after 24 h at r.t.

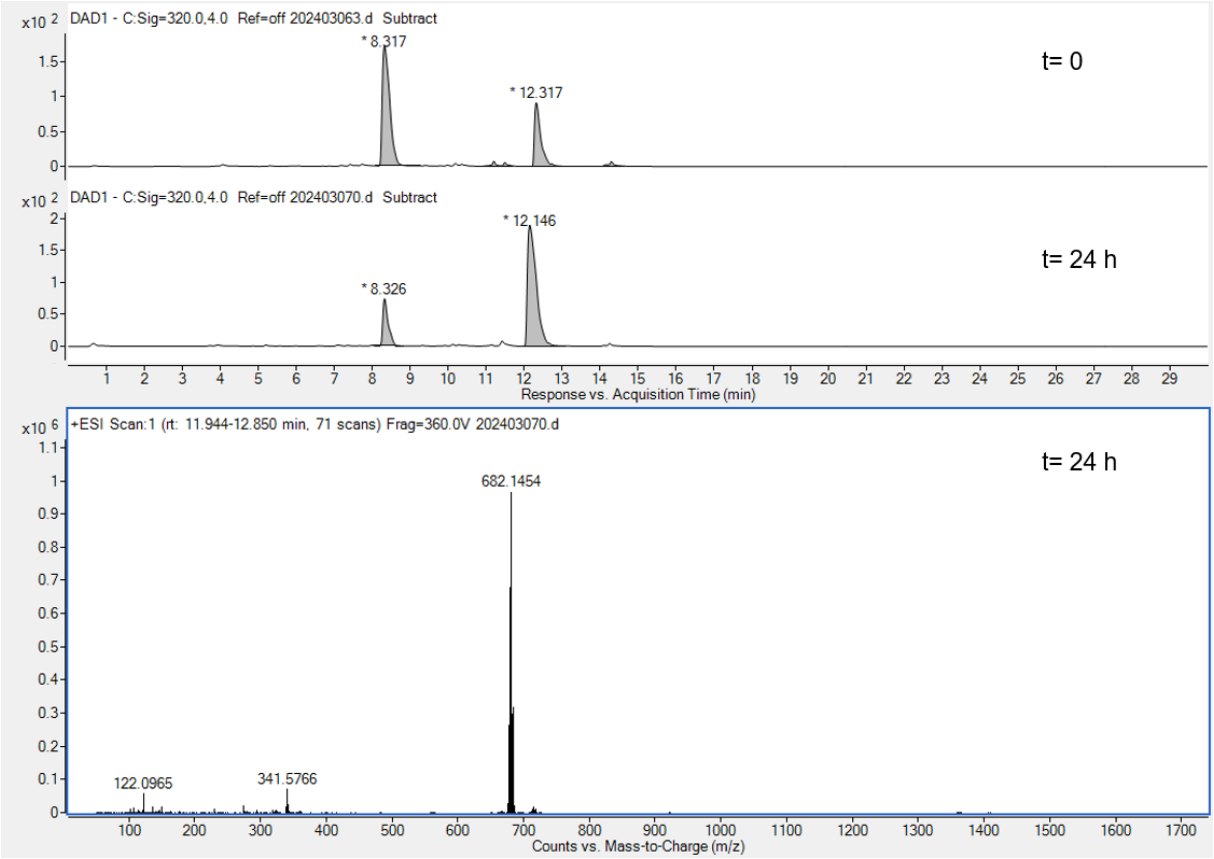

Figure S46. HPLC-MS of **Os5** (10 μM) in RPMI (5 % DMSO) at t=0 and after 24 h at r.t.

8. Interaction with Biomacromolecules

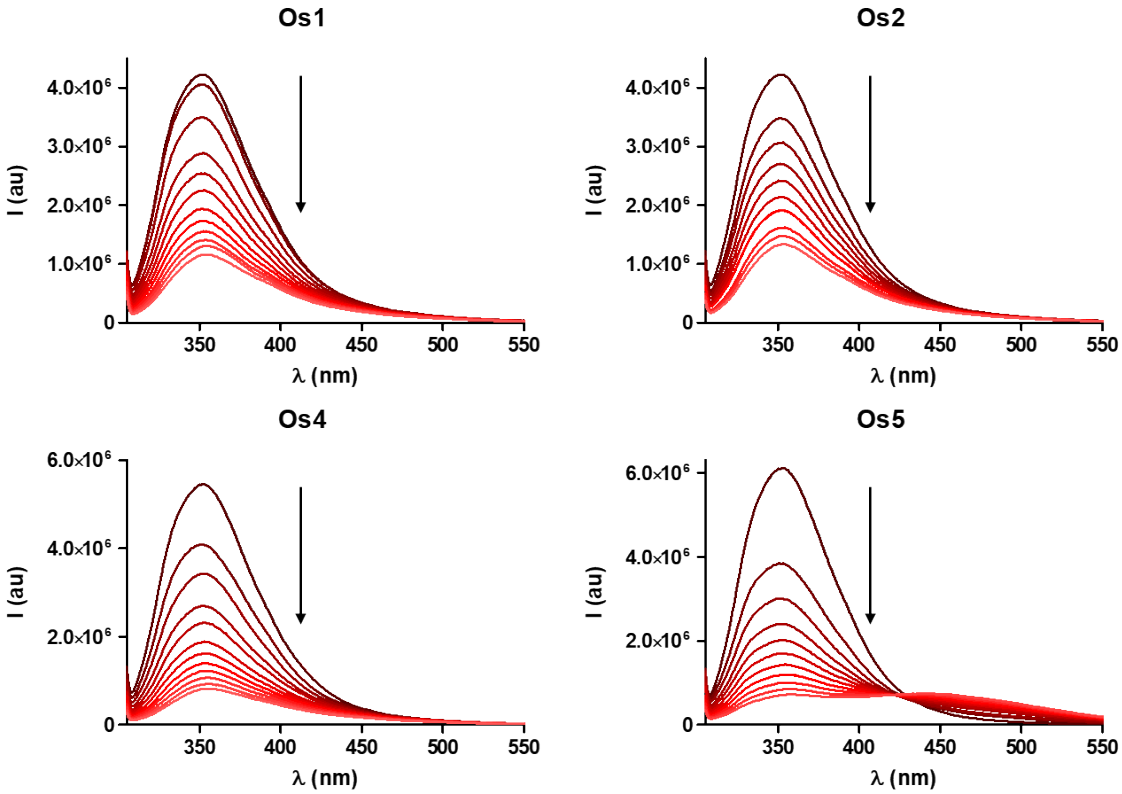

Figure S47. Emission spectra of HSA (2.7 μM) in the presence of increasing amounts of **Os1-Os5** complexes (0-27 μM) from top to bottom.

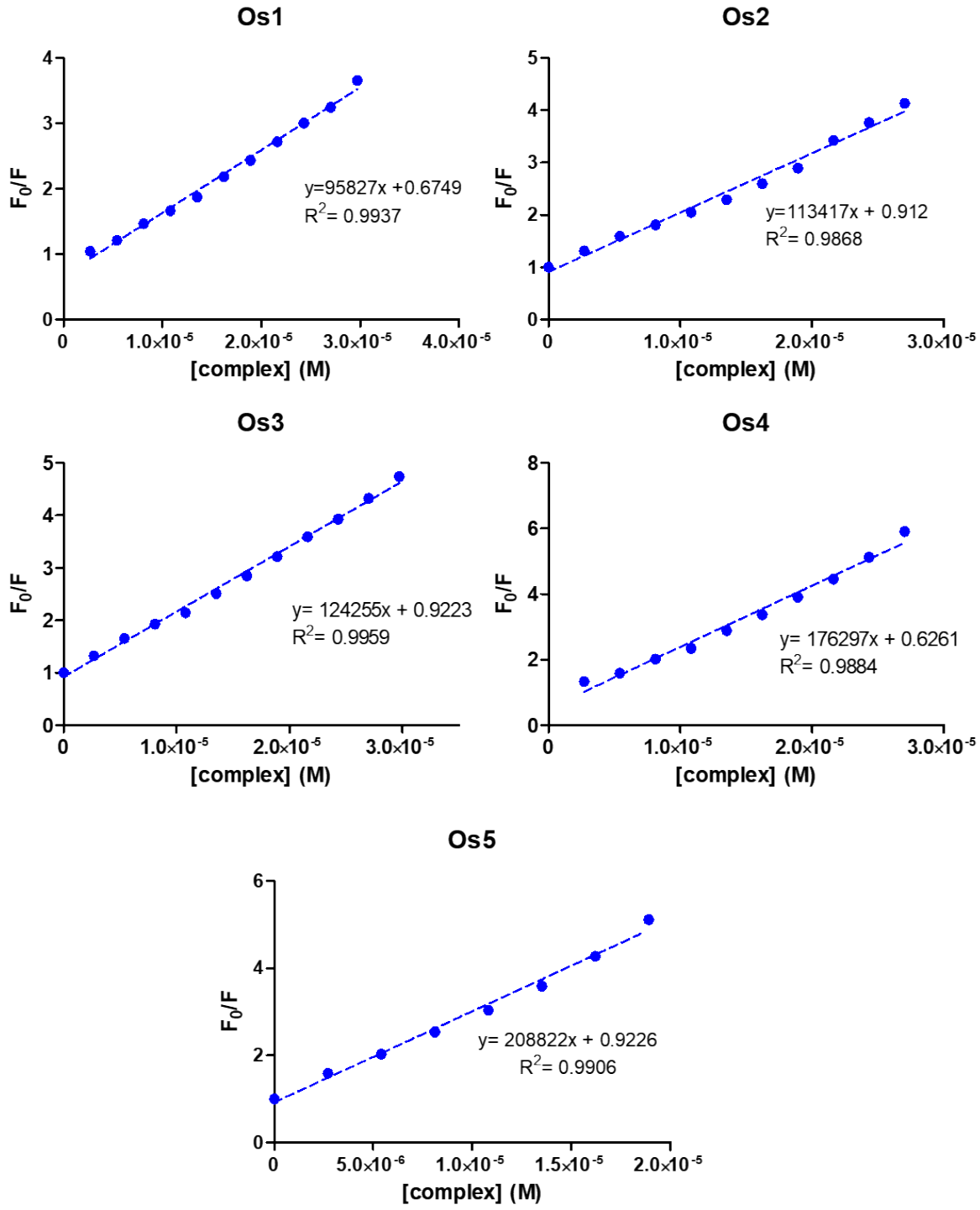

Figure S48. Stern-Volmer plots of the quenching of HSA fluorescence in the presence of **Os1-Os5** complexes.

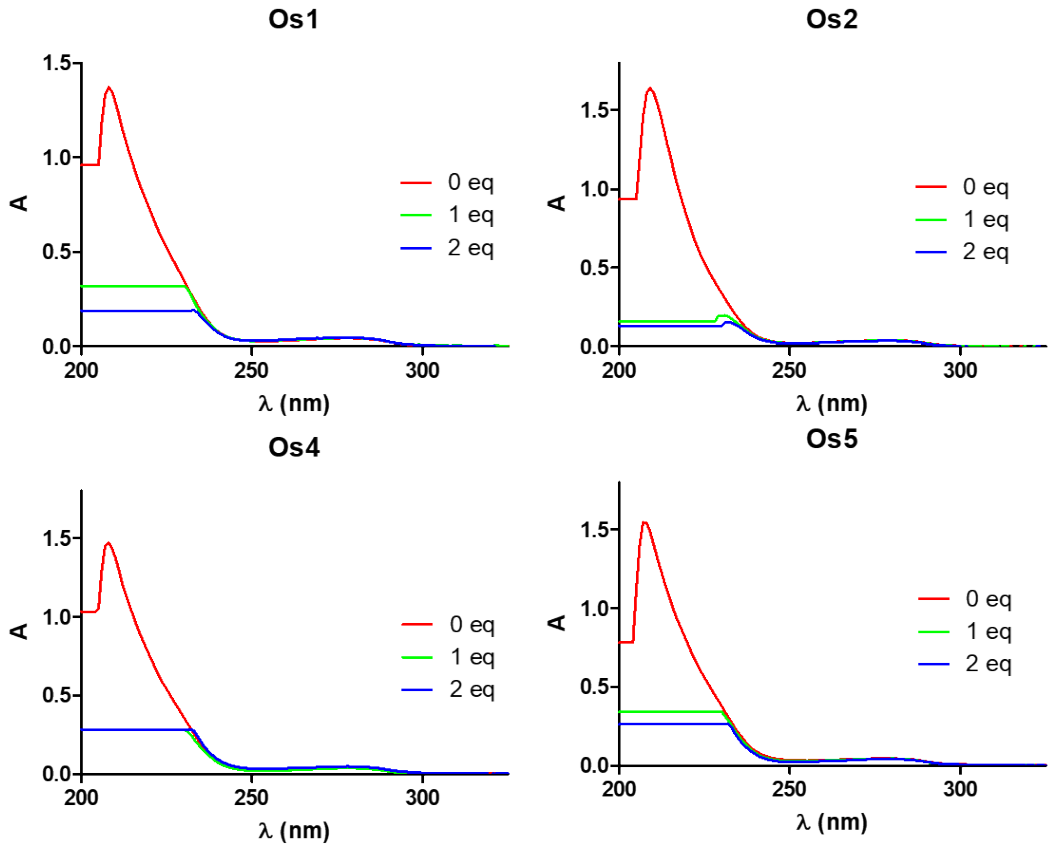

Figure S49. UV/visible spectra of HSA (1 μM) with increasing amounts of **Os1-Os5** (0-2 eq).

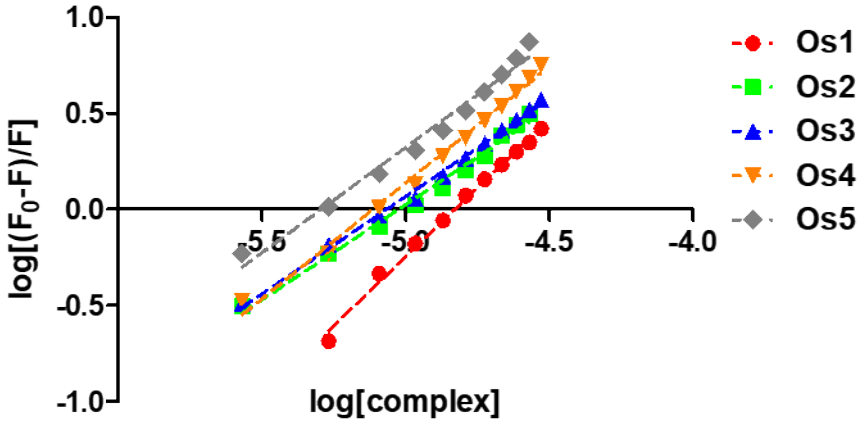

Figure S50. Scatchard plots of the quenching of HSA fluorescence in the presence of **Os1-Os5** complexes.

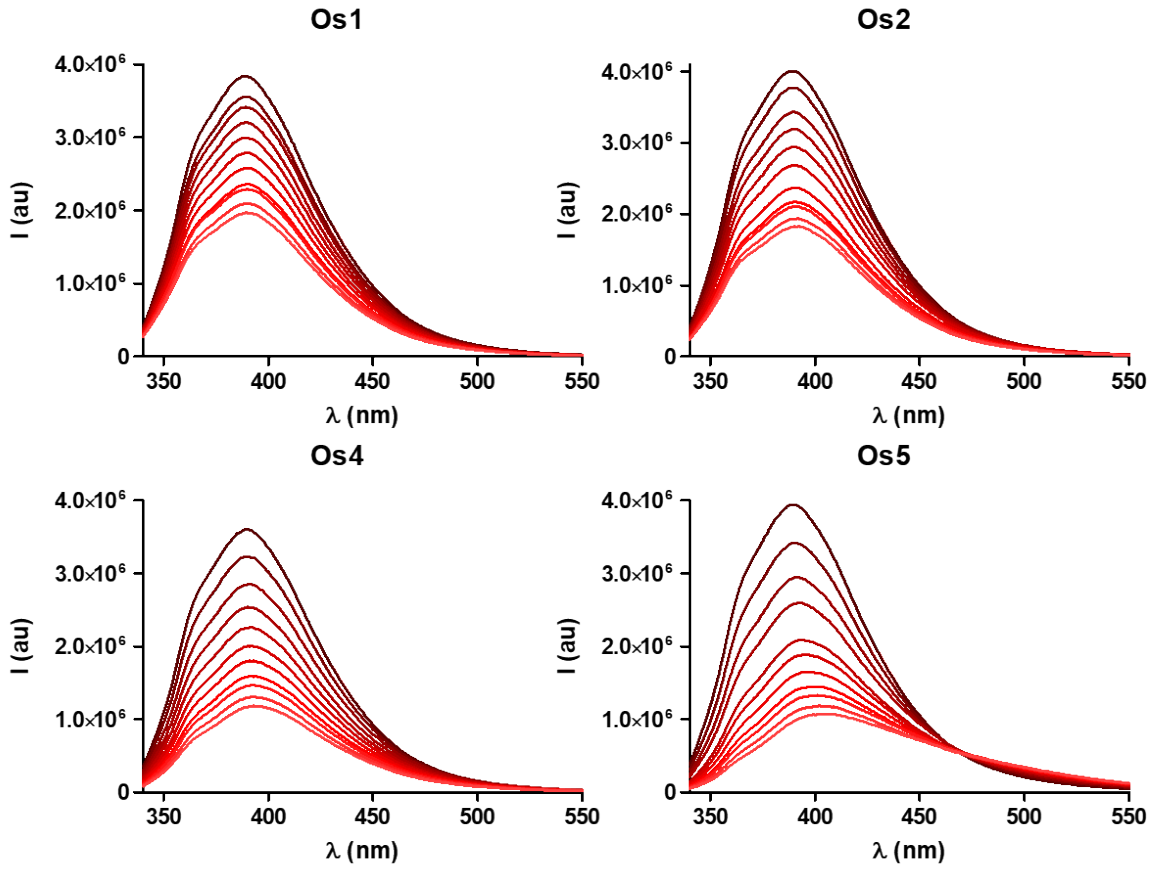

Figure S51. Emission spectra of HSA-WF in the presence of increasing amounts of complexes **Os1-Os5** (0-25 μM). λ_{ex}= 320 nm, [HSA-WF]= 1.0:1.0 μM. (top to bottom gradual increments).

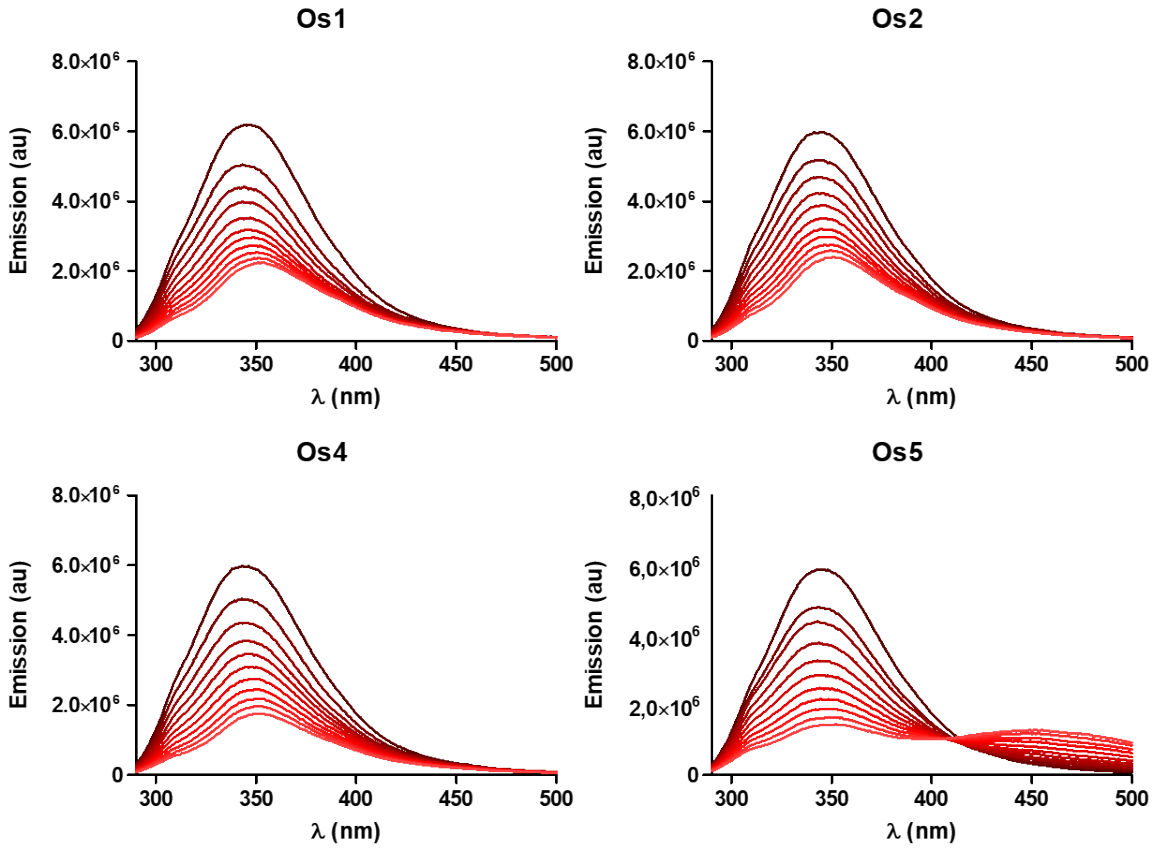

Figure S52. Emission spectra of HSA-IBU in the presence of increasing amounts of complexes (0-25 μM). λ_{ex}= 280 nm, [HSA-IBU]= 1.0:1.0 μM. [Complexes]: 0-25 μM (top to bottom gradual increments).

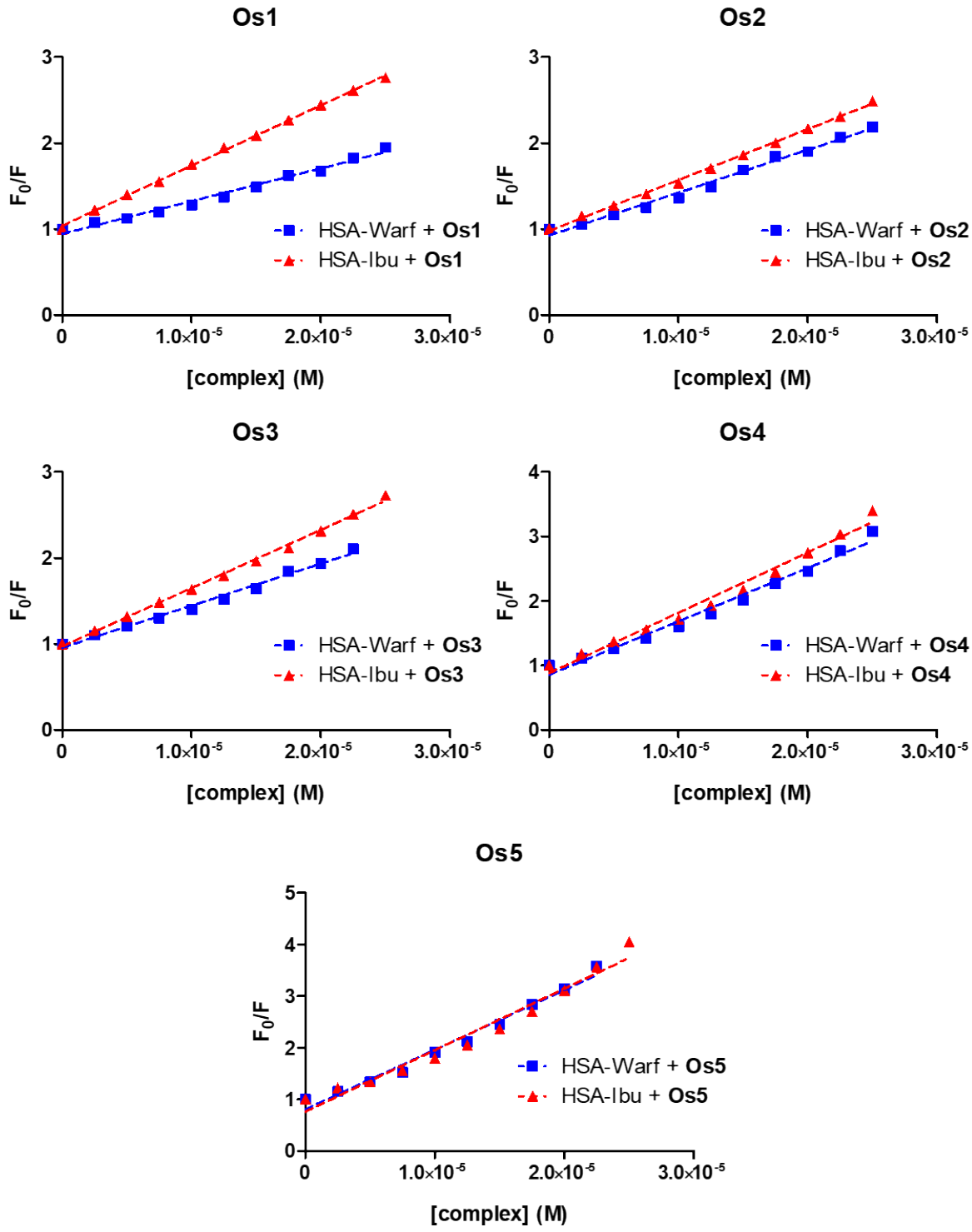

Figure S53. Stern-Volmer plots of the quenching of [HSA-WF] or [HSA-IBU] fluorescence in the presence of **Os1-Os5** complexes.

9. Biological assays

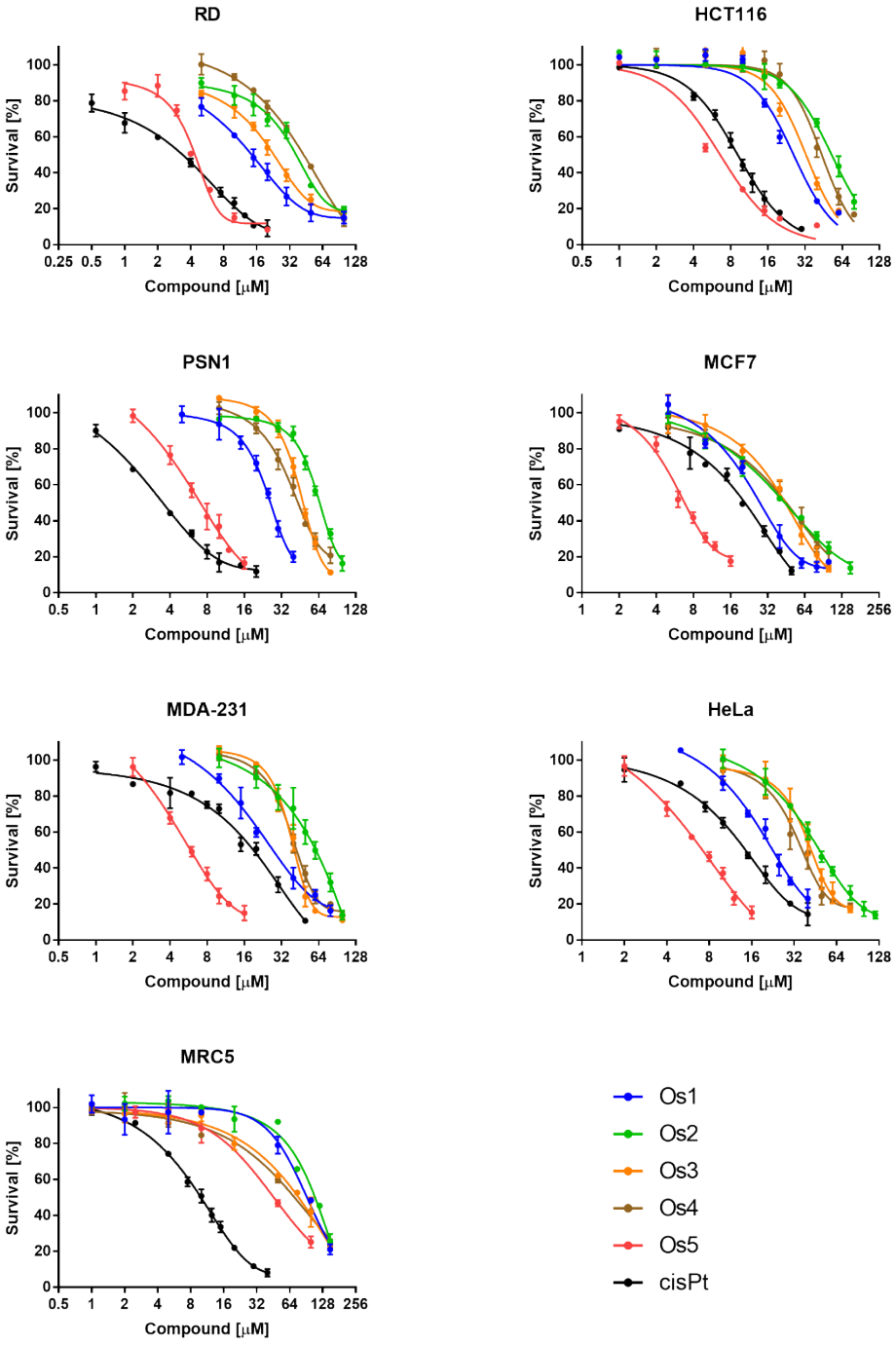

Figure S54. Representative dose-response curves as obtained by MTT assay.

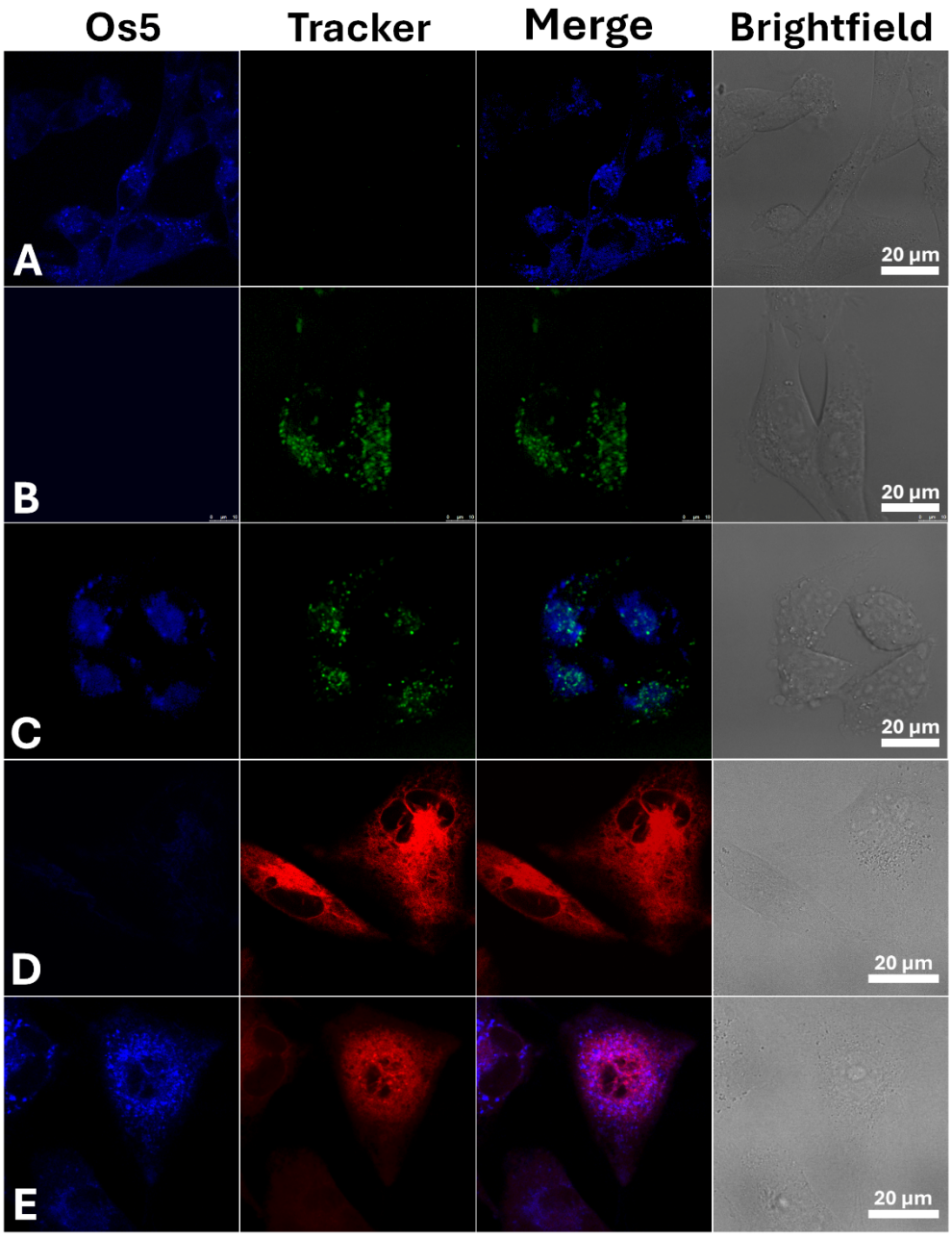

Figure S55. Colocalization of **Os5** in Rhabdomyosarcoma cells with lysosomes and endoplasmic reticulum. The cells were prestained with Lyso-Tracker or ER-Tracker and then exposed to **Os5** (12.9 µM) for 1 h. **Os5** (Blue) – the signal of **Os5**; Tracker – the signal of either Lyso-Tracker (B, C) or ER-Tracker (D, E); Merge – the merged signal of **Os5** and the specific tracker; Brightfield – brightfield channel. (A) – Cells exposed only to **Os5**; (B) – cells exposed only to Lyso-Tracker; (C) – cells exposed to **Os5** and Lyso-Tracker; (D) - cells exposed only to ER-Tracker; (E) - cells exposed to **Os5** and ER-Tracker.

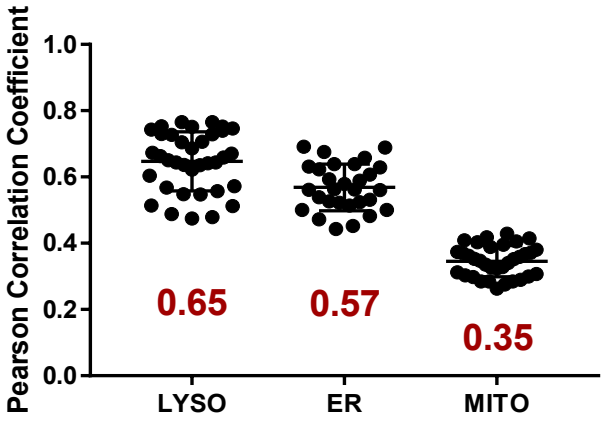

Figure S56. Colocalization of **Os5** with ER-Tracker, Lyso-Tracker, and TMRE. The correlation coefficients were calculated from images obtained with RD cells pretreated with individual trackers and treated with **Os5** for 1 h. The red number represents an average of correlation coefficients determined with ImageJ software.

Table S10. Percentual distribution of Os from **Os5** in cellular fractions of RD cells.

Cellular fraction	**Percentual distribution[a]**
Cytosolic	21±4
Membrane/Particulate	71±6
Nuclear (proteins and membrane)	6.3±0.9
Cytoskeletal+DNA	1.7±0.3

[a]RD cells were incubated with 50 μM Os5 for 5 hours. The cells were then processed with FractionPREP™ Cell Fractionation kit to obtain four cellular fractions. Osmium content in individual fractions was determined with ICP-MS. Two samples were analyzed, and the results are shown as MEAN±SD.

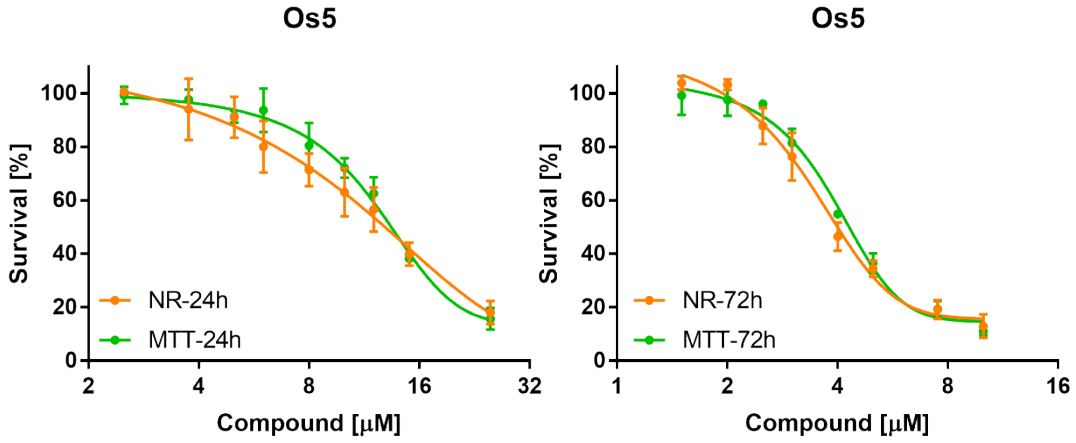

Figure S57. Representative dose-response curves as obtained by MTT and NR assays.

Table S11. IC_{50} values (μM). IC_{50} values were determined in CD133+ and CD133- RD cells using Cell TiterGlo 3D assay.

IC_{50} (μM)[a,b]	Os1	Os2	Os3	Os4	Os5	cisPt	Sal	CF
RD.CD133-	19 ± 2	30 ± 6	24 ± 3	47 ± 3	3.9 ± 1.2	12 ± 3	0.8 ± 0.2	592 ± 90
RD.CD133+	12 ± 4	27 ± 5	17 ± 2	45 ± 6	3.1 ± 0.8	15 ± 3	0.5 ± 0.1	455 ± 90

[a]The spheroids were treated for 72 h.

[b]Data represents MEAN±SD from at least three independent experiments.

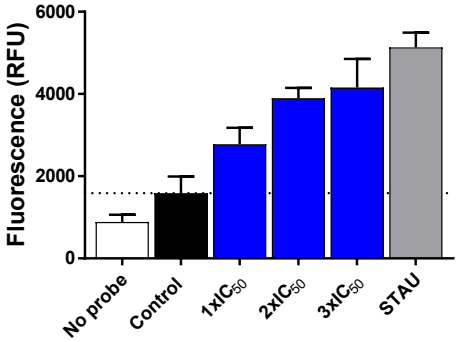

Figure S58. Caspase-3 activation detected with CellEvent® Caspase3/7 Green Detection Reagent. RD cells were treated with vehicle or **Os5** at concentrations corresponding to 1x, 2x, and 3xIC_{50} values for 24 h. STAU – cells were treated with staurosporine (2 μM) for 3 hours. Following the staining with the green reagent (30 min), the cells were analyzed with flow cytometry. $2x10^4$ cells were analyzed per run; the experiment was performed twice. The results are represented as MEAN±SD. Student t-test confirmed statistically significant differences from non-treated control for all treated samples with $p \leq 0.01$ or $p \leq 0.001$.

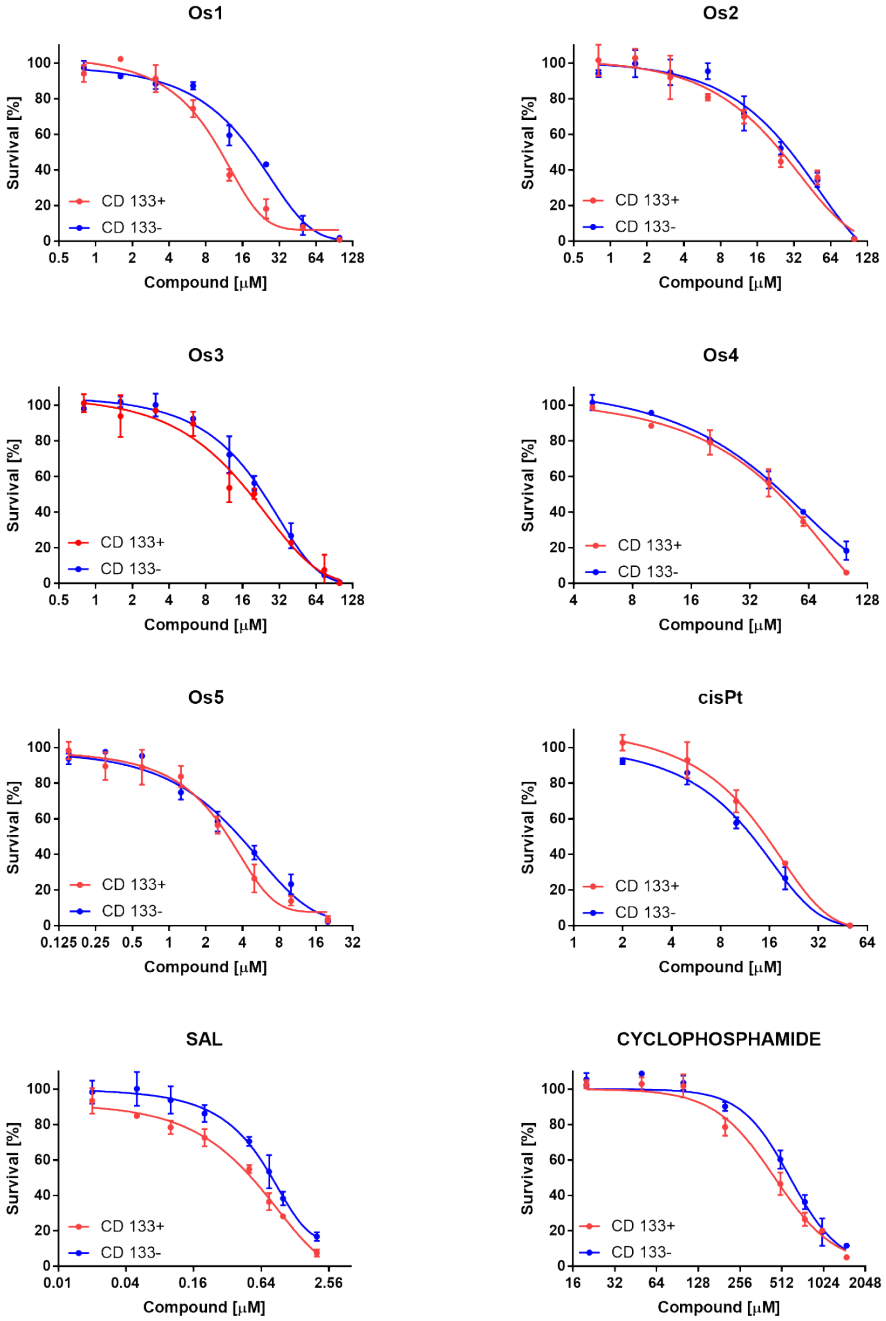

Figure S59. Representative dose-response curves as obtained by Cell TiterGlo 3D assay.

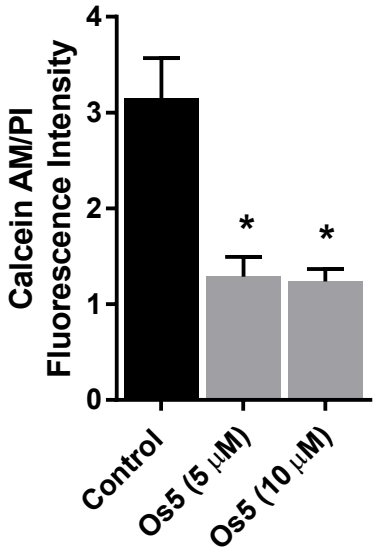

Figure S60. Quantification of confocal microscopy images. The graph shows ratios of Calcein AM fluorescence intensity to PI fluorescence intensity in untreated spheroids (Control) and spheroids exposed to **Os5** for 72 h. Fluorescence intensities were measured with ImageJ software. Three spheroids were scored per sample. The asterisks denote significant differences from untreated control as determined with the Student t-test (p<0.01).